
Performance of Brownian Motors

Zur Erlangung des akademischen Grades eines
Doktors der Naturwissenschaften
der Mathematisch–Naturwissenschaftlichen Fakultät
der Universität Augsburg vorgelegte

Dissertation

von

Łukasz Machura

aus

Zawiercie

Augsburg, im Januar 2006

Betreuer:

Prof. Dr. Peter Hänggi
Theoretical Physics I
University of Augsburg, Germany

Prof. Dr. Peter Talkner
Theoretical Physics I
University of Augsburg, Germany

Prof. Dr. Jerzy Łuczka
Department of Theoretical Physics
University of Silesia, Katowice, Poland

Erster Bericht:	Prof. Dr. Peter Hänggi
Zweiter Bericht:	Prof. Dr. Jerzy Łuczka
Tag der mündlichen Prüfung:	15 März 2006

Contents

1	Introduction	5
2	Stochastic model of a tilted rocked ratchet	13
2.1	Langevin equation	13
2.2	Scaling	14
2.3	Fokker-Planck Equation	14
2.4	Potential Profiles	16
2.5	Numerical method	17
3	Quantifiers characterizing the optimal transport	19
3.1	Effective Diffusion and Péclet number	19
3.2	Rectification Efficiency	19
4	Zero bias force	23
4.1	Generic Ratchet	23
4.1.1	Deterministic dynamics	23
4.1.2	Noisy dynamics: Fluctuations versus driving strength	27
4.1.3	Noisy dynamics: Fluctuations versus noise strength	32
4.2	Optimization of the performance	36
5	Inertial motor under load	41
5.1	Biasing the ratchet	41
5.1.1	Current-load behavior	41
5.1.2	Efficiency of forced and rocked Brownian motors	42
5.2	Absolute negative mobility in a symmetric potential	43
6	Summary	49
A	Effective Diffusion	51
B	Efficiency	53
	Bibliography	55

1 Introduction

Isn't it sometimes that a facade
of randomness and chaos
conceals a demon
of order and harmony.

(Łuczka)

Historical remarks

In 1827 Robert Brown (1773–1858), a leading British botanist observed under the microscope irregular motion of pollen grains and spores of mosses suspended in water (see Fig. 1.1) ¹. Puzzled by the phenomenon he performed a number of further experiments, using different organic and inorganic objects, different surrounding fluids like water or alcohol and different microscopes. One year later he published his findings [1] where he concluded that this kind of motion is caused by the bombardments by the small particles, which he calls "active molecules". His theory, however, has one weakness: He claimed that the motion of active molecules originates from the molecules themselves and not that it is caused by heat. He knew that he was not the first to discover this kind of mobility and in his 1829 paper [2] he referred to a number of experiments and observations done earlier, however, for organic bodies only. Although Brown was not the first observer of this kind of motion, he was the pioneering experimentalist who made systematic investigations, trying to understand the origin of this random motion. His study showed that this kind of motion is universal and in particular not restricted to living matter. He turned the story of the neverending inanimate bodies dances in fluids from biology to a problem of physics. Brown was not aware of the work of the Dutch physiologist, botanist and physicist Jan Ingen-Housz (1730–1799), who in 1785 had made some observations of the irregular motion of carbon dust on alcohol.

After Brown other scientists performed their own experiments and proposed new theories, in order to give a quantitative description of the phenomenon. Unfortunately, the experimentalists usually measured the instantaneous velocities of the frisky particles and ended up with irreproducible average values. There were also several attempts to explain of this kind of motion, mostly as an effect of external forces, like the most popular temperature gradient produced by the light illuminating the probe and the convection connected with it.

The breakthrough came with Albert Einstein (1879–1955) in his *annus mirabilis* 1905, when he published, beside others outstanding papers, his theoretical explanation of Brownian

¹ The picture of Robert's Brown microscope (Fig. 1.1) used on the courtesy of Prof. Brian J. Ford (<http://www.brianjford.com>).



Figure 1.1: Robert Brown's microscope as presented to the Linnean Society in 1928 [3].

motion in [4]. This work has provided an evidence for the existence of atoms, and moreover, directed the experimentalists to what they should focus in their experiments on the Brownian motion, namely, to the fluctuations of position of a Brownian particle. He derived there the famous formula for the relation between the diffusion coefficient D and osmotic pressure for the particle of radius r suspended in a liquid at the temperature T . He showed that D is related to the Boltzmann constant k_B (i.e to the ratio of the ideal gas constant R and the Avogadro number N_A) and molecular dimension via the Stokes friction γ (or equivalent the coefficient of the viscosity of solvent η) [5]. Nowadays, in a statistical physics, this formula is referred to as the *Einstein relation*

$$D = \frac{RT}{N_A} \frac{1}{6\pi\eta r} = \frac{k_B T}{\gamma}. \quad (1.1)$$

Also in 1905, William Sutherland (1859–1911) developed similar theory yielding the same formula for the coefficient of diffusion [6]. At the same time Marian Smoluchowski (1872–1917), also worked on the kinetic theory of Brownian motion. He used a different approach – his derivation was based on combinatorics and the mean free path approximation. In 1906, provoked by Einstein's publication, he presented his own work, where he proposed the equation which later on became the basis of the theory of stochastic processes [7, 8].

Three years after Einstein's elaboration, the French physicist Paul Langevin (1872–1946) devised a very different technique of description of the Brownian motion, in his own words "infinitely more simple" than Einstein's. By introducing a stochastic (complementary) force representing the random "kicks" in the velocity space, he solved the problem by means of Newton's second law. Einstein used the method of deriving and solving partial differential (Fokker-Planck) equation for the time evolution of the probability density of position of the Brownian particle (i.e. the diffusion equation).

It is however surprising that Einstein and Langevin used the term "Brownian motion", but did not cite any paper of Robert Brown and instead referred to the experiments by the French physicist Léon Gouy [9].

The experimental confirmation of the kinetic theories of Brownian motion came with Jean Baptiste Perrin (1870–1942) [10], who won the 1926 Nobel Prize for his work on the discontinuous structure of matter.

The two approaches, based on the Fokker-Planck and the Langevin equations, are now widely used as the equivalent formulation of continuous Markov processes in many different branches of science like physics, chemistry, economy and even in social sciences.

Ratchet introduced

In 1912 Smoluchowski published a paper [11] where he designed in a thought experiment a gadget showing the possibility of rectifying thermal energy using a ratchet and pawl mechanism. In other words - he proposed a device that far from the equilibrium state is able to convert the thermal motion of Brownian particles into directed motion, just by using the breaking of symmetry. The small section in [11] was like a kind of response to the postulate of L. Gouy who had insinuated that the molecular ratchet mechanism would violate the second law of thermodynamics [12]. The same idea was reformulated and elucidated in the early 1960 by Richard Feynman (1918–1988) in his famous "Lecture of Physics" [13].

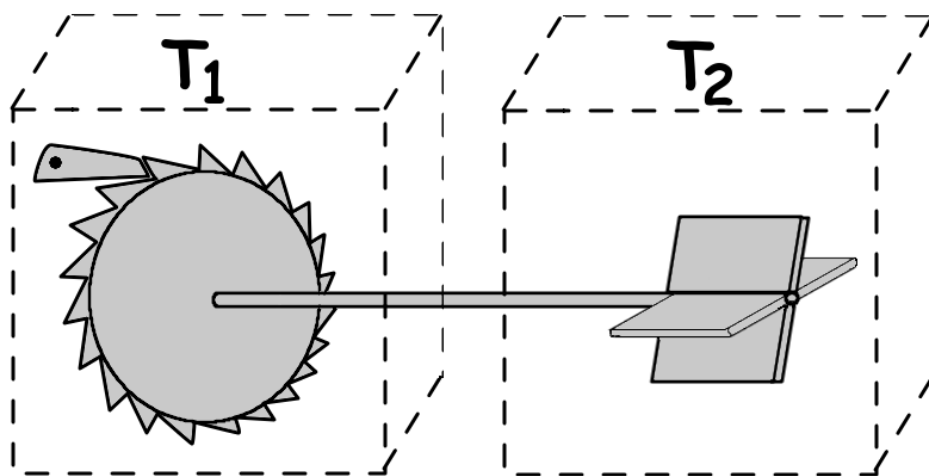


Figure 1.2: A schematic cartoon of the Smoluchowski-Feynman ratchet and pawl device.

Let us briefly examine the apparatus we call Smoluchowski-Feynman ratchet presented in the Fig. 1.2. The machine consists of an axle with vanes at one of its ends and a ratchet at the other. The pawl restricts the motion in one direction. Both ends of the instrument placed in

different "boxes" with gas temperatures T_1 and T_2 , undergo random motion due to collisions with molecules. The first impression is that at even the same temperatures $T_1 = T_2$, the axle may only turn in one direction because of the pawl mechanism and on the average a directed motion is generated by means of the thermal fluctuations. It looks like that we have just constructed a *perpetuum mobile* of the second kind or a specific Maxwell demon is seemingly at work. The paradox was explained by Feynman [13]: Every single part of the device is subjected to the neverending bombardments of equal intensity in all directions. It is therefore possible that due to the Brownian motion, the pawl would rise above the ratchet's teeth and cause turns in both directions with the same probability. The net motion is then obviously zero. A critical analysis of the Smoluchowski-Feynman construction is presented in [14, 15]. On the other hand, if the two temperatures are different, $T_1 \neq T_2$, the resulting average motion is nonzero. In this case, the macroscopic difference of temperature causes the net motion of the axle.

This analysis can be a motivation for an abstract mathematical formulation [16] of the *ratchet device* illustrated in Fig 1.2:

- a) The ratchet (wheel) presents a spatially periodic system. It corresponds to a spatially periodic potential $V(x) = V(x + L)$.
- b) The symmetry of the ratchet is broken, because of the pawl mechanism (the teeth are asymmetrical). It corresponds to a breaking of a reflection symmetry of the potential: there is no real number x_0 , such that the relation $V(x_0 - x) = V(x_0 + x)$ is fulfilled.
- c) The average random force acting on the vanes and caused by collisions of gas molecules is zero. It corresponds to the zero-mean thermal fluctuations.
- d) The directed motion can be induced by a temperature gradient or a constant bias force. However, these are trivial cases and instead we would drive the system out of the equilibrium state with a nonthermal force of a zero mean.

Since Feynman the knowledge of the physics of ratchets was put forward. There exists a very rich literature dealing with the above formulated issue [17, 18], mainly in the overdamped regime [19]. There are many conceptual models of ratchets including pulsating ratchets with a deterministic driving [20–22], random dichotomic driving [23, 24] or deterministic driving but a dichotomic random force [25]. Moreover, the fluctuating force ratchets with random dichotomic [26, 27], Gaussian tilting [28–30], rocking (periodic tilting) ratchets or asymmetric tilting ratchets (assuming spatially symmetric potential but asymmetric driving) was also studied. Other possibilities of extracting useful motion from zero-mean forces are extensions of the Smoluchowski-Feynman device – temperature ratchets with periodic temperature variations [31] or dichotomous random switching of the temperature [26, 32–34]. The ratchet effect was found also for a case of inhomogeneous (state dependent) friction [35, 36]. There exists also an amazing phenomenon that makes use of the ratchet effect, called *Parrondo paradox* [37–39]. If we refer to the configuration of the system as to a game and we consider two

fair games, we can express this paradox as the following: by random switching between two fair random games one can end up with a game that is no longer fair.

Another important family of ratchet-based systems are molecular motors. The name refers to proteins or protein complexes that are able to transduce chemical energy, usually stored in the ATP (AdenosineTriPhosphate), into mechanical work and directed motion in an asymmetric environment at the molecular scale. There are transporting proteins (translational motors) which move along the intracellular, polar “highways”, like tubulin filaments (with kinesin walking towards the positive and dynein to the negative end) or active filaments (with corresponding myosin advancing in the positive extremity). The filaments are asymmetric and periodic structures with period of about $8nm$. Other motor proteins perform rotatory motions, like the F_1F_0 ATPase which produces (with nearly 100% efficiency [40, 41]) the life-essential nucleotide ATP. It is stunning that every day we produce and burn a half of our body weight in ATP. In fact it is not at all easy to move in a cellular environment. Due to the relatively high viscosity of the surrounding fluid the motor has to struggle against the strong friction force. On the other hand due to the heat bombardments by particles of the solution the motor perceives strong kicks in every direction. For the molecular motor it is like to “walk in a hurricane and swim in molasses” [42, 43].

Many different aspects of the molecular motors were studied in great detail. The model of a motor with two feet and its manner of walking (stepping) along tubulin was addressed both experimentally [44–46] and theoretically [47–52]. A one dimensional model of the motor in an open tube, with dynamics alternating between two configurations, when the motor moves on a tubulin using the ratchet effect (bounded state) and the free diffusive motion in the tube (unbounded state) was studied in [53–55]. The mechanical properties of a motor was examined by use of an optical tweezers technique [56–58] and the conformational changes of a motor simulated by means of molecular dynamics [59], to name but a few.

The overdamped dynamics is a valid approximation for many physical applications [60]. It is particularly well suited to describe the motion of molecular motors. In other situations the inertial effects, however, can play an important role. Examples are the diffusion of adatoms on a crystal surface [61–63], dissipation in threshold devices [64, 65], dislocation of defects in metals [66, 67] and in a hysteretic Josephson junction [68, 69].

Subject of this thesis

In this thesis we will study transport of an *inertial* Brownian particle in a periodic ratchet-type potential additionally subjected to an external, time periodic force, i.e. rocked ratchet. The vast majority of works focused on rocking ratchets is concentrated on the behavior of the *overdamped* regime [70–72] and the control of the emerging directed transport as a function of control parameters such as temperature, external load (yielding the load-current characteristics), or some other control variable, for reviews see [17, 18, 43, 73–76].

A notable exception is the first work on an inertial rocking ratchet [77] wherein the higher-order, statistical cumulant properties of the stochastic position variable have been explored. The deterministic aspects of the inertial rocked dynamics has extensively been studied within the last few years. We give a short review of the present state of art in the section 4.

In contrast, the role of the fluctuations of the directed current has not attracted much attention in the literature [62]. Here, we fill this gap and focus in more detail on the fluctuating behavior of the Brownian motor position and current. The average drift motion together with its fluctuation statistics are salient features when characterizing the performance of a Brownian motor.

When we study the motion of Brownian motors, the natural transport measure is a conveniently defined average asymptotic velocity $\langle\langle v \rangle\rangle$ of the Brownian particle. It describes how much time a typical particle needs to overcome a given distance in the asymptotic (long-time) regime. This velocity, however, is not the only appropriate transport criterion and other attributes can also be important.

The goal of this work is to constitute the most significant characteristics relevant for optimization of the Brownian motor *modus operandi*. In order to establish them, we consider the two following aspects: the quality of the transport and the energetic efficiency of such a system.

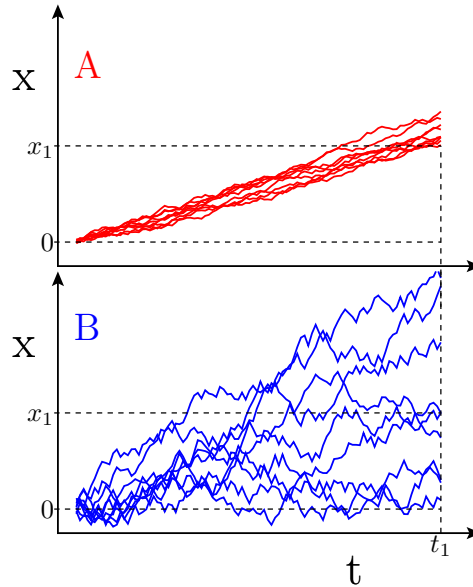


Figure 1.3: Two sets of illustrative trajectories of an inertial, rocked Brownian motor (see in text). Both sets of trajectories A and B possess the same average asymptotic velocity, but exhibit a distinct different diffusion behavior.

In Fig. 1.3, one can identify two different groups A and B of random trajectories of the Brownian particle; both possess the same average drift velocity $\langle\langle v \rangle\rangle$. However, it is obvious upon inspection that the dynamical properties of these two groups of trajectories are different. The particles from the group A travel more or less coherently together while the particles from the group B spread out as time goes by. If we fix the distance $x = x_1$ then most particles from the group A reach this distance at about the same time $t = t_1$, while most of the B trajectories

either stay behind or have already proceeded to more distant positions. It is thus evident that the noise-assisted, directed transport for the particles in the group A is more organized than in the group B.

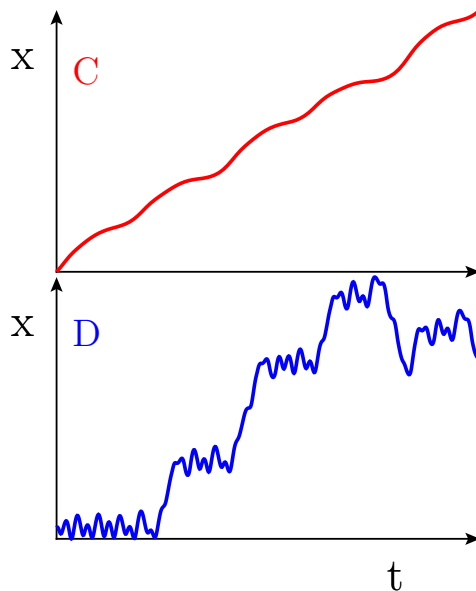


Figure 1.4: Typical trajectories of an inertial, rocking Brownian motor; both sets assume the same average velocity but differing velocity fluctuations.

There is still another aspect related to Brownian motor transport. This refers to the external energy input into the system which may be essential in practical applications. We would like to know how much of this input energy is converted into useful work, namely into directed cargo transport, and how much of it gets wasted. Since motors move in a dissipative environment, we need to know how much of the input energy is being spent for moving a certain distance against the acting friction force. If the particle additionally proceeds against a bias force we can also ask how much energy is exploited for this purpose.

Fig. 1.4 depicts trajectories representing different motor scenarios. The motor C moves forward unidirectionally. The motor D moves in a more complicated manner: its motion alternates between small oscillations and fast running episodes mostly in the positive x direction, but sometimes also in the opposite one. Again the mean velocity in both cases is the same, however, the particle C uses energy pumped from the environment to proceed constantly forward while the particle D wastes part of its energy to perform oscillations and back-turns. By simply inspecting these schematic pictures one can guess immediately when directed transport is more effective.

We note that in Fig. 1.3, the cases A and B can be characterized by the effective diffusion coefficient D_{eff} , i.e., by the spreading of fluctuations in the position space at a fixed time while the cases C and D in Fig. 1.4 can be characterized by the variance of velocity $\sigma_v^2 =$

$\langle\langle v^2 \rangle\rangle - \langle\langle v \rangle\rangle^2$. The three quantities $\langle\langle v \rangle\rangle$, D_{eff} and σ_v^2 can be combined to define two important characteristics of transport, namely the efficiency of noise rectification [78, 79] and the so-called Péclet number [80–83].

Outline

The thesis is organized as the following: In the next chapter we present the typical model of tilted rocked Brownian particle, its dimensionless form and the potential profiles used in this work. Next, in the second chapter we discuss the quantifiers of interest. In the chapter 4 we present the result of the numerical analysis of the unbiased, noisy inertial dynamics and identify the optimal driving parameters of the discussed system. In the chapter 5 the inertial biased rocked dynamics is addressed. In the last chapter we summarize the thesis.

2 Stochastic model of a tilted rocked ratchet

The archetype of the inertial Brownian motor is represented by a classical particle of mass m moving in a spatially periodic potential $V(x) = V(x + L)$ with period L and barrier height ΔV [77, 84]. The particle is driven by an external, unbiased, time-periodic force of amplitude A and angular frequency Ω (or period $\mathcal{T}_\Omega = 2\pi/\Omega$). The system is additionally subjected to the thermal noise $\xi(t)$ and the constant load force F . The thermal fluctuations due to the

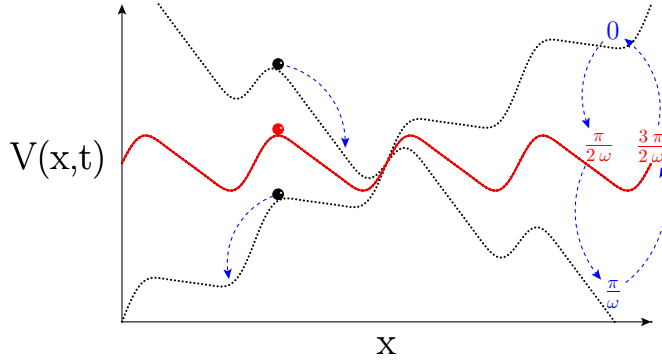


Figure 2.1: Schematic picture of a rocking ratchet with the potential $V(x,t) = V(x) - xa \cos(\omega t)$, cf. Eqs (2.3) with zero bias ($F = 0$) and a ratchet potential $V(x)$ defined in (2.19).

coupling of the particle with the environment are modeled by a Gaussian white noise $\xi(t)$ of a zero mean

$$\langle \xi(t) \rangle = 0 \quad (2.1)$$

and the auto-correlation function satisfying Einstein's fluctuation-dissipation relation

$$\langle \xi(t)\xi(s) \rangle = \delta(t - s). \quad (2.2)$$

We mentioned in the introduction that there are two equivalent descriptions of stochastic dynamics. One is the Langevin equation of motion that describes the time evolution of a position $x(t)$ and a velocity $v(t)$ of the Brownian particle. The second is the Fokker–Planck equation that describes the time evolution of a probability density $P(x, v, t)$.

2.1 Langevin equation

The dynamics of the system is modeled by the Langevin equation [85]

$$m\ddot{x} + \gamma\dot{x} = -V'(x) + F + A \cos(\Omega t) + \sqrt{2\gamma k_B T} \xi(t), \quad (2.3)$$

where a dot denotes differentiation with respect to time and a prime denotes a differentiation with respect to the Brownian motor coordinate x . The parameter γ denotes the Stokes friction coefficient, k_B stands for the Boltzmann constant and T is the temperature.

2.2 Scaling

Upon introducing characteristic length- and time-scales, Eq. (2.3) can be rewritten in dimensionless form, namely

$$\ddot{\hat{x}} + \hat{\gamma}\dot{\hat{x}} = -\hat{V}'(\hat{x}) + \hat{F} + a \cos(\omega\hat{t}) + \sqrt{2\hat{\gamma}D_0} \hat{\xi}(\hat{t}), \quad (2.4)$$

with [78]

$$\hat{x} = \frac{x}{L}, \quad \hat{t} = \frac{t}{\tau_0}, \quad \tau_0^2 = \frac{mL^2}{\Delta V}. \quad (2.5)$$

The characteristic time τ_0 is the time a particle of mass m needs to move the distance $L/2$ under the influence of the constant force $\Delta V/L$ when starting with a zero velocity. The remaining re-scaled parameters are:

- the friction coefficient $\hat{\gamma} = (\gamma/m)\tau_0 = \tau_0/\tau_L$ is the ratio of the two characteristic times, τ_0 and the relaxation time of the velocity degree of freedom, i.e., $\tau_L = m/\gamma$,
- the potential $\hat{V}(\hat{x}) = V(x)/\Delta V = \hat{V}(\hat{x} + 1)$ has unit period and unit barrier height $\Delta\hat{V} = 1$,
- the load force $\hat{F} = FL/\Delta V$,
- the amplitude $a = AL/\Delta V$ and the frequency $\omega = \Omega\tau_0$ (or the period $\mathcal{T} = 2\pi/\omega$),
- the zero-mean white noise $\hat{\xi}(\hat{t})$ has auto-correlation function $\langle \hat{\xi}(\hat{t})\hat{\xi}(\hat{s}) \rangle = \delta(\hat{t} - \hat{s})$ with re-scaled noise intensity $D_0 = k_B T/\Delta V$.

From now on, for the sake of simplicity, we will use only the dimensionless variables and shall omit the “hat” for all quantities in Eq. (2.4).

2.3 Fokker-Planck Equation

The statistically equivalent Fokker-Planck equation corresponding to eq. (2.4) describing the time evolution of the probability density $P(x, v, t)$ is given by the formula

$$\frac{\partial}{\partial t} P(x, v, t) = L_{FP}(t) P(x, v, t), \quad (2.6)$$

with the time periodic Fokker-Planck operator

$$L_{FP}(t) = -\frac{\partial}{\partial x}v - \frac{\partial}{\partial v}\left[F - \gamma v - V'(x) + a \cos(\omega t)\right] + \gamma D_0 \frac{\partial^2}{\partial v^2}, \quad (2.7)$$

$$L_{FP}(t + \mathcal{T}) = L_{FP}(t). \quad (2.8)$$

Using the Fokker-Planck equation (2.6) with the given initial conditions we get the probability density $P(x, v, t)$ and define the averages

$$\langle g(x(t), v(t)) \rangle = \int dx \int dv g(x, v) P(x, v, t), \quad (2.9)$$

e.g. the n -th moment of the position $x(t)$

$$\langle x^n(t) \rangle = \int dx \int dv x^n P(x, v, t). \quad (2.10)$$

The integration of $P(x, v, t)$ over the position x of the particle defines the time dependent velocity distribution

$$P(v, t) = \int dx P(x, v, t), \quad (2.11)$$

and as a consequence the mean velocity

$$\langle v(t) \rangle = \int dv v P(v, t). \quad (2.12)$$

For large times the periodically driven stochastic process approaches an asymptotic periodic velocity probability distribution $P_{as}(v, t)$ (the positive and periodic function of time),

$$P_{as}(v, t + \mathcal{T}) = P_{as}(v, t), \quad (2.13)$$

with normalization

$$\int dv P_{as}(v, t) = 1. \quad (2.14)$$

The asymptotic averages can be then defined as

$$\langle g(v(t)) \rangle_{as} = \int dv g(v) P_{as}(v, t), \quad (2.15)$$

so the asymptotic average velocity is given by

$$\langle v(t) \rangle_{as} = \int dv v P_{as}(v, t). \quad (2.16)$$

For later use we introduce the time averaged asymptotic velocity distribution

$$P_{as}(v) = \frac{1}{\mathcal{T}} \int_0^{\mathcal{T}} dt P_{as}(v, t), \quad (2.17)$$

and the time averaged mean velocity

$$\langle\langle v \rangle\rangle = \frac{1}{\mathcal{T}} \int_0^{\mathcal{T}} dt \langle v(t) \rangle_{as} = \lim_{t \rightarrow \infty} \frac{1}{t} \int_0^t ds \langle v(s) \rangle. \quad (2.18)$$

2.4 Potential Profiles

For the asymmetric ratchet potential $V(x)$ we consider the linear superposition of three spatial harmonics [78],

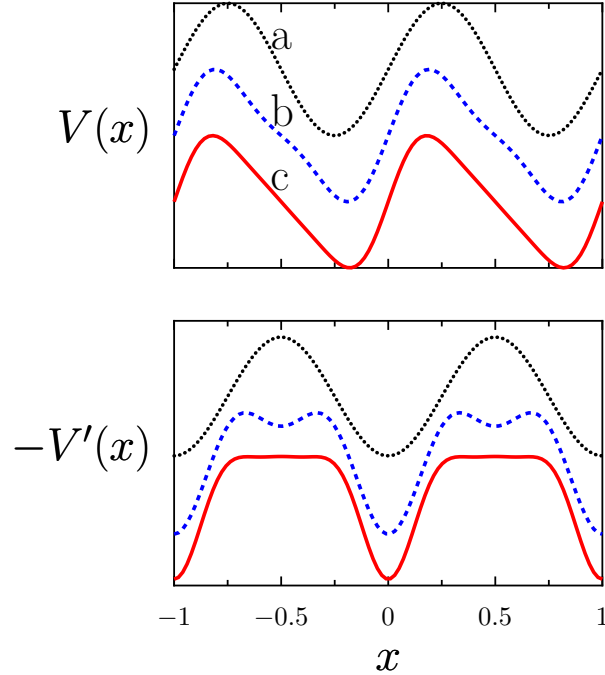


Figure 2.2: A plot of the shape of the periodic potential $V(x)$ and corresponding force $F(x) = -V'(x)$ defined in (2.19) for:

- a) a symmetric sinus potential $c_1 = c_2 = 0$ (dotted);
- b) an asymmetric ratchet potential $c_1 = 0.25, c_2 = 0$ (dashed);
- c) an asymmetric ratchet potential $c_1 = 0.245, c_2 = 0.04$ (solid).

To illustrate the differences, the potentials and corresponding forces was shifted up or down for the cases a) and c), respectively.

$$V(x) = V_0[\sin(2\pi x) + c_1 \sin(4\pi x) + c_2 \sin(6\pi x)], \quad (2.19)$$

where V_0 normalizes the barrier height to unity and the parameters c_1 and c_2 determine the ratchet profile (or the spatial asymmetry – see Figure 2.2). In this work we analyze the following cases:

- a) the simple sinus potential:

$$c_1 = 0, c_2 = 0 \quad \rightsquigarrow \quad V_0 = 0.5$$

- b) the ratchet profile:

$$c_1 = 0.25, c_2 = 0 \quad \rightsquigarrow \quad V_0 \approx 0.454,$$

c) the ratchet profile:

$$c_1 = 0.245, c_2 = 0.04 \quad \rightsquigarrow \quad V_0 \approx 0.461.$$

There is also a possibility to extract the effective force acting on the molecular motor and therefore reproduce the corresponding effective ratchet potential. One can perform this calculation by means of the analysis of the time series [86] using the recorded single-molecule experimental data [40, 56]. In this thesis, however, we will deal with the three hypothetical potential profiles given above.

2.5 Numerical method

The noiseless, deterministic inertial rocked ratchet shows rather complex behavior and, in distinct contrast to overdamped rocked Brownian motors, often exhibits a chaotic dynamics. By adding noise, one typically obtains a diffusive dynamics, thus allowing stochastic escape events among possibly coexisting attractors.

As analytical methods to handle these situations effectively do not exist, we carried out extensive numerical simulations. We have numerically integrated Eq. (2.4) by the Stochastic Runge Kutta (SRK) method of the second order [87] with time step $h = 10^{-3}$ – $10^{-4} \mathcal{T}$. The initial conditions for the coordinate $x(t)$ were chosen according to a uniform distribution within one cell of the ratchet potential. The starting velocities of the particles were also distributed uniformly in the interval $[-0.2, 0.2]$.

The first 10^3 periods \mathcal{T} of the external force were skipped in order to eliminate transient effects. For the estimation of the quantities of interest the usual averages over the time ($10^6 \mathcal{T}$) and 333 different realizations were taken.

When simulating the deterministic equation (4.3) one has to choose among the several possibilities of initiations of runs. By doing this one has to be sure, that computed averages are relevant and do not differ much for another set of initial conditions. If there is only one attractor present (like e.g. the case shown on the Fig. 5.3) for given driving parameters we need only one run *de facto*. If there are more attractors the calculated quantities can vary for the different sets of initial conditions due to an often fractal structure of the basins of attraction. However, one can enlarge the number of runs and compare the calculated quantifiers for this different sets. We did this for five different forms of uniform distributions of the initial conditions:

- $x = x_0$ and $v \in [-0.2, 0.2]$, where x_0 is a position of the local minimum of the spatial periodic potential,
- $x \in [0, L]$ and $v = 0$,
- $x \in [0, L]$ and $v \in [-0.2, 0.2]$,
- $x \in [0, L]$ and $v \in [-2, 2]$,
- a circle in the phase space with the origin at $(x,v)=(x_0,0)$ and radius $r = 0.2$.

2 *Stochastic model of a tilted rocked ratchet*

We have increased the number of runs up to the point where we have obtained the satisfactory agreement of maximal 1% difference between the calculated averages of the specific quantity (e.g. velocity $\langle\langle v \rangle\rangle$) for the above given sets of initial conditions.

3 Quantifiers characterizing the optimal transport of Brownian motors

As already elucidated in the introduction, there are several quantities that characterize the effectiveness of directed transport [88]. A global transport measure is an asymptotic mean velocity $\langle\langle v \rangle\rangle$ of the Brownian motor averaged over one cycle of the external, time periodic drive and over all noise realizations, see eq. (2.18).

3.1 Effective Diffusion and Péclet number

The effective diffusion coefficient, describing the fluctuations around the average position of the particles, is defined as

$$D_{eff} = \lim_{t \rightarrow \infty} \frac{\langle x^2(t) \rangle - \langle x(t) \rangle^2}{2t}, \quad (3.1)$$

The coefficient D_{eff} can also be introduced via a generalized Green-Kubo relation, which we detail in Appendix A. Intuitively, if the stationary velocity is large and the spread of trajectories is small, the diffusion coefficient is small and the transport is more effective. To quantify this, we can introduce the dimensionless ratio – the Péclet number Pe [80, 81, 89] by use of a double-averaging procedure, i.e.,

$$Pe = \frac{l \langle\langle v \rangle\rangle}{D_{eff}}, \quad (3.2)$$

Originally, the Péclet number Pe has arisen in problems of heat transfer in fluids and stands for the ratio of heat advection to diffusion [89]. When the Péclet number is small, the random motion dominates; when it is large, the ordered and regular motion prevails. The value of the Péclet number depends on a characteristic length scale l of the system. Dealing with ratchets the most adequate choice for such length scale is the period of the periodic potential, which in re-scaled units (see section 2.2) is equal to $l = 1$.

3.2 Rectification Efficiency

The second aspect of the motor trajectories we want to control is related to the fluctuations of the velocity $v(t)$. In the long-time regime, it is characterized by the variance $\sigma_v^2 = \langle\langle v^2 \rangle\rangle - \langle\langle v \rangle\rangle^2$. The Brownian motor moves with an actual velocity $v(t)$, which is typically contained within the interval

$$v(t) \in (\langle\langle v \rangle\rangle - \sigma_v, \langle\langle v \rangle\rangle + \sigma_v). \quad (3.3)$$

Now, if $\sigma_v > \langle\langle v \rangle\rangle$, the Brownian motor may possibly move for some time in the direction opposite to its average velocity $\langle\langle v \rangle\rangle$ and the directed transport becomes less efficient.

If we want to optimize the effectiveness of the motor motion we must introduce a measure for the efficiency η that accounts for the velocity fluctuations. Assume, that the motor works against the given force \mathcal{F} (not yet define). The efficiency of a machine is defined as the ratio of the power $P = \mathcal{F}\langle\langle v \rangle\rangle$ done on the surroundings and the input power P_{in} , $\eta = P/P_{in}$. If the motor is working against the constant external load force F , one can define the *efficiency of energy conversion* [18, 75, 76, 86, 90, 91]; reading,

$$\eta_E = \frac{|F\langle\langle v \rangle\rangle|}{P_{in}}. \quad (3.4)$$

A grave disadvantage of such a characterization is that it yields a vanishing measure (i.e. $\eta_E = 0$) in the absence of a load force F . In many cases, however, like e.g. for protein transport within a cell, the Brownian motor operates at a zero bias regime ($F = 0$) and its objective is to carry a cargo across a viscous media. Clearly, the energy input required to move a particle with the friction coefficient γ by a given distance depends on the velocity, tending to zero at slow motion. Since we are interested in delivering the cargo in a finite time one should require that the transport is accomplished at an average motor velocity $\langle\langle v \rangle\rangle$. In this case, the necessary energy input is finite. Thus, we put for \mathcal{F} the average viscous force $\gamma\langle\langle v \rangle\rangle$ to obtain the so-called *Stokes efficiency* [86, 92]; i.e.,

$$\eta_S = \frac{\gamma\langle\langle v \rangle\rangle^2}{P_{in}}. \quad (3.5)$$

There is no overall consensus on the numerator in (3.5) [79, 90–100]. If we put in the numerator the rate of work done on the fluid by the Brownian motor motion, then the corresponding efficiency η_S is not an appropriate measure because numerator is $\simeq \langle v^2 \rangle$. This quantity can be relatively large even if there occurs no transport of the motor, i.e. even if $\langle v \rangle = 0$! More suitable information on the efficiency of the transport is gained when [92, 96] the numerator $\simeq \langle v \rangle$, as proposed here. Upon combining the two above given notions we recover the *rectification efficiency* originally proposed by Suzuki and Munakata [79, 101] or its equivalent version presented by Derenyi *et al.* [96]

$$\eta_R = \frac{\gamma\langle\langle v \rangle\rangle^2 + |F\langle\langle v \rangle\rangle|}{P_{in}}. \quad (3.6)$$

It is made up of the sum of the efficiencies η_S and η_E . Therefore, it accounts for both, the work that the Brownian motor performs against the external bias F as well as the work that is necessary to move the object a given distance in a viscous environment at the average velocity $\langle\langle v \rangle\rangle$.

The average input power for a tilted rocking ratchet is given by [78, 82]:

$$P_{in} = \gamma|\langle\langle v^2 \rangle\rangle - D_0|. \quad (3.7)$$

This expression follows from an energy balance of the underlying equation of motion (2.4). The derivation of the above formula can be found in Appendix B. If the second moment of velocity $\langle\langle v^2 \rangle\rangle$ is reduced, i.e. the variance σ_v diminishes, the rectification efficiency (3.6) increases and the transport of the Brownian motor becomes more efficient.

To experimentally determine either of the above given efficiencies of any molecular motor (like kinesin) it is sufficient to determine the average velocity of the motor with its variance and the temperature of the thermal bath [102].

4 Performance with zero bias force

In this chapter we put the constant bias force of the driven system (2.4) equal to zero ($F = 0$). It means that there is no apparent preferred direction of the Brownian particle to travel. The dynamics is now governed by the following equation of motion:

$$\ddot{x} + \gamma\dot{x} = -V'(x) + a \cos(\omega t) + \sqrt{2\gamma D_0} \xi(t). \quad (4.1)$$

We would like to identify conditions for the optimal performance of the above defined rocking ratchet. We follow the arguments given in the introduction and search for the operation regimes where the whole set of particles would advance in a coherent manner, utilizing as much of the input energy as possible for a directed motion, without back turns or intrawell oscillations.

For the overdamped dynamics given by

$$\gamma\dot{x} = -V'(x) + a \cos(\omega t) + \sqrt{2\gamma D_0} \xi(t). \quad (4.2)$$

we can identify two thresholds of the external force strengths: the lower threshold a_{c1} and the upper threshold a_{c2} . The first corresponds to the force that is needed to overcome the barrier of the potential from the side with the smaller slope. The second threshold corresponds then to the force that the particle needs to overcome the barrier of the potential from side with the steeper slope. Note that for the inertial dynamics these two strengths are not that relevant, since the particle can accumulate kinetic energy and therefore is able to make a transition over one of the barriers of the ratchet potential for weaker driving strengths than a_{c1} or a_{c2} .

4.1 Generic Ratchet

The roots of the noisy ratchet effect lie in the evolution of the Newton equation (eq. (4.1) with $D_0 = 0$). First of all we recall the analysis of the deterministic dynamics of a particle moving in a typical ratchet profile, widely investigated in the literature [77, 103–115].

4.1.1 Deterministic dynamics

As the generic ratchet potential we take the one that consist of two spatial harmonics (i.e. $c_2 = 0$, see Fig. 2.2 (b)). The corresponding Newton equation reads

$$\ddot{x} + \gamma\dot{x} = -2\pi(\cos(2\pi x) + \frac{1}{2} \cos(4\pi x)) + a \cos(\omega t). \quad (4.3)$$

Since we have an explicit time dependence, the phase space is three dimensional. The nonlinearity of the noiseless equation (4.3) then allows chaotic attractors to appear. For the attractor that takes a particle along n spatial periods L of potential in k time periods \mathcal{T}

$$\begin{aligned} v(t + k\mathcal{T}) &= v(t), \\ x(t + k\mathcal{T}) &= x(t) + nL, \end{aligned} \tag{4.4}$$

we can define the winding number W as a ratio

$$\overline{W} = \frac{n}{k}. \tag{4.5}$$

For locked orbits the particle stays in one well of potential forever and therefore $n = 0$ and corresponding winding number is also $W = 0$. For running solutions the winding number can assume any number, depending on the dynamics. This measure corresponds to the characteristic average velocity of a particle being translocating by a given attractor

$$\bar{v} = \frac{nL}{k\mathcal{T}} = W \frac{L}{\mathcal{T}}. \tag{4.6}$$

If we reduce the system to an overdamped one (cf. eq. (4.2) with $D_0 = 0$), the dimensionality of the state space become two and it prevents the particle to act in a chaotic manner.

In the Fig. 4.1 we show stroboscopically the instantaneous velocities of the deterministic particles with different starting conditions (for details see section 2.5) and therefore we plotted all attractors existing at a given value of a control parameter a . As a stroboscopic time interval we took the period of the driving force \mathcal{T} . We plot this so-called bifurcation diagram as a function of the driving strength a . To eliminate transient effects 10^6 periods \mathcal{T} of the external driving were disregarded. Other parameters of the system (4.3) are fixed to the values: $\gamma = 0.5$ and $\omega = 3.6$.

For small driving strengths a the massive particle possesses not enough kinetic energy to make a transition over any barrier of the ratchet potential. As we increase a the particle can eventually accumulate enough kinetic energy to go over one of the barriers and running solutions emerge. Therefore, for small values of a the transport is regular. If we increase the control parameter for values larger than $a = 1.8$ we can notice several transitions from a regular periodic motion to chaos and back from chaos to a periodic motion. At the bifurcation point $a_b \simeq 2.33$ the transition from chaotic to regular, periodic attractor of period four occurs (this point is indicated by an arrow in Fig. 4.1). Note that for the noisy dynamics (cf. Fig. 4.3), we reveal the first current reversal at this very point $a \simeq 2.33$. Very close to this bifurcation point the deterministic system exhibits intermittent dynamics of type I (cf. the second column in Fig. 4.2) [116, 117] reflecting the reciprocation of one chaotic and one periodic attractors [103]. For smaller values than a_b , say for $a = 2.25$ there exists one periodic orbit of period one, that transports the particles in the negative x direction, cf. the first column in Fig. 4.2. For $a = 2.25$ the particle cross $n = 1$ spatial period in $k = 1$ time period so the winding number $W = 1$ and characteristic velocity $\bar{v} = 3.6/2\pi$. For a stronger than a_b , say for $a = 2.35$,

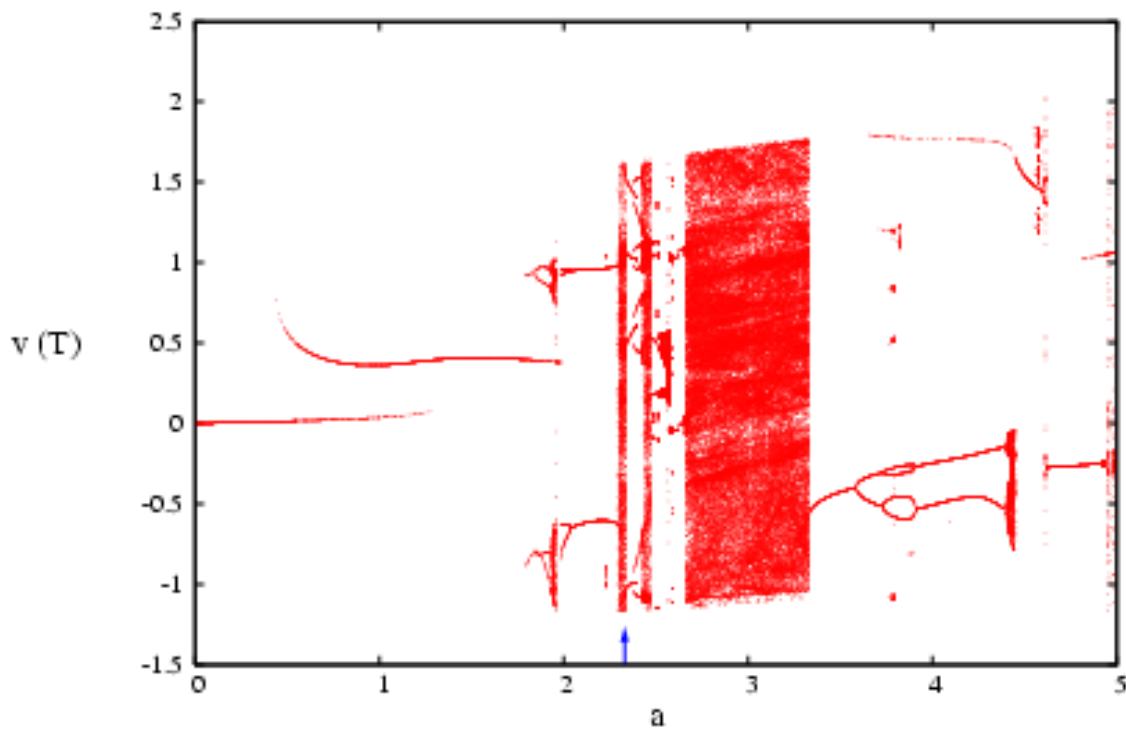


Figure 4.1: Bifurcation diagram: stroboscopic velocity v as a function of periodic driving strength a , plotted for a potential shown in Fig. 2.2 (b). For a given value a we show all existing attractors. The arrow indicates the bifurcation point from chaos to period 4 attractor at $a = 2.33$, see text for details. The remaining rescaled parameters read: friction $\gamma = 0.5$, angular driving frequency $\omega = 3.6$.

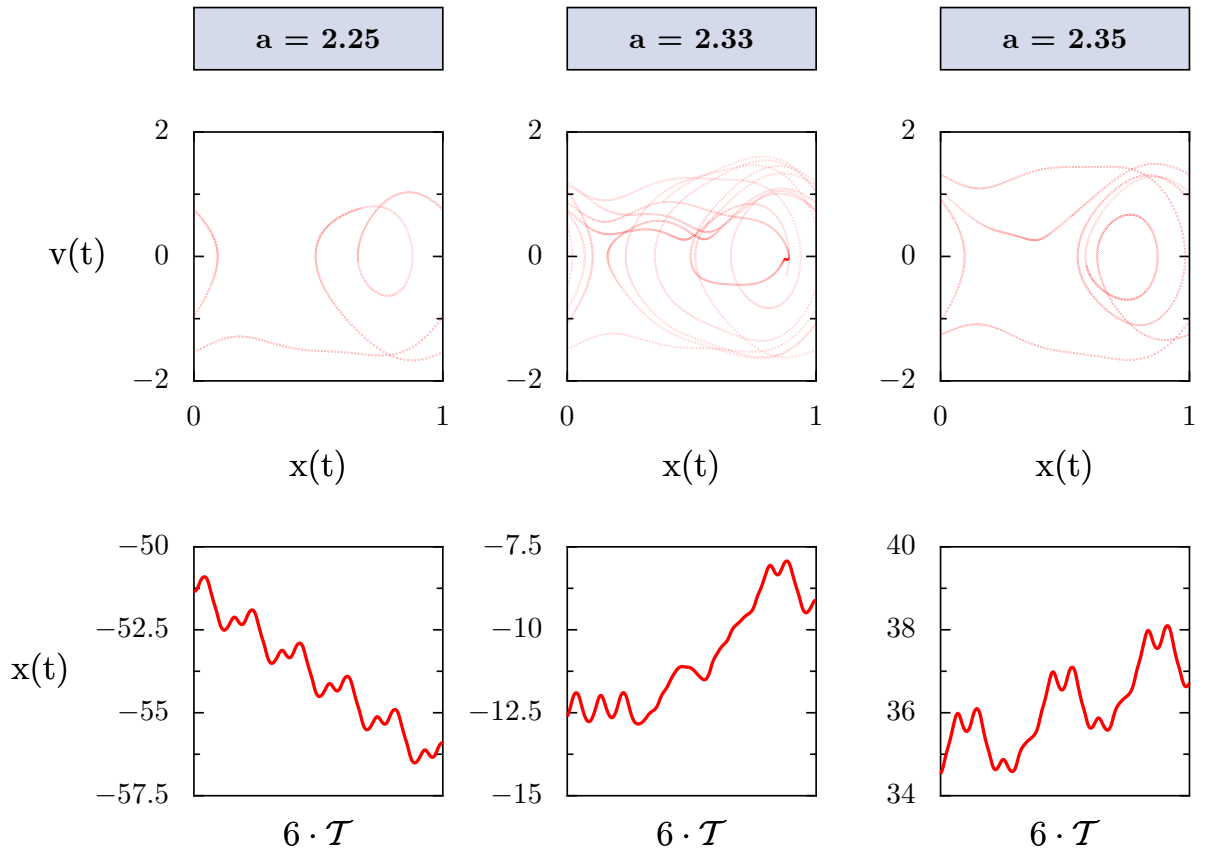


Figure 4.2: Deterministic motion shown for the same set of parameters as in the Fig. 4.1 and the three driving strengths $a = 2.25, 2.33, 2.35$.

Upper row: The phase space (instantaneous velocity versus position). For $a = 2.25$ one can note the negative periodic attractor of period one \mathcal{T} ; for $a = 2.33$ the intermittent chaotic attractor emerge; for $a = 4.6$ the positive, period two regular attractor is shown.

Lower row: Trajectories of the particles shown as an illustration of the attractors plotted in the upper row for a time interval $6\mathcal{T}$.

after the bifurcation point, we find one regular attractor (see the third column in Fig. 4.2) that transports the particle in the positive x direction over $n = 1$ period of potential in $k = 2$ time periods and therefore the winding number $W = 1/2$ and $\bar{v} = 3.6/4\pi$. In general: If the corresponding pre- and post-bifurcation attractors can transport the particles in the opposite directions then it is likely that after the bifurcation point the current reversal appears.

Due to very complicated structure of the basins of attraction it is however not clear how to compute averages in the deterministic case and e.g. the mean velocity would strongly depend on the chosen set of initial conditions. For some sets of control parameters and depending on the initial conditions, we can reveal multiple attractors in the phase space. Again, if they can transport the particle in the opposite direction, we would gain the possibility of separate particles, by choosing the appropriate attractor via its basin of attraction i.e. by choosing the appropriate starting conditions [112].

Plugging the noise into the system, one get rid of this problem, allowing the Brownian particle to visit all existing attractors, depending on the noise intensity but independent of the initial conditions. In the following we deal with a relatively low temperature of the heat bath so the deterministic architecture of attraction still affects the noisy driven dynamics (4.1).

4.1.2 Noisy dynamics: Fluctuations versus driving strength

We start out to study the role of fluctuations in both position and velocity space, by varying the amplitude a of the sinusoidal driving force. In doing so, we assume a relatively small temperature, so that the Brownian motor dynamics is not far from a deterministic behavior as described in prior works. To put it all into numbers, we choose the following set of the parameters: friction $\gamma = 0.5$, angular driving frequency $\omega = 3.6$ and weak thermal noise of strength $D_0 = 0.01$. The average asymptotic long-time velocity is shown in Fig. 4.3 (a). It reveals that for an amplitude $a \simeq 1.5$ the directed, *inertial* transport sets in before the lower threshold of the ratchet force $a_{c1} \simeq 2.14$ is reached. The mean velocity assumes a first local extremum near the lower threshold of the potential force $a \simeq a_{c1}$. Note that in the presence of small noise, the current is strictly speaking never zero. However, the noise induced transitions over the potential barriers for a weak driving strength are extremely rare and the system mainly dwells in the locked state, so we can characterize the outcome of our Langevin simulation as a deterministic, zero-current result. Upon closer inspection, we notice that in the vicinity of $a \simeq 0.6$, the velocity fluctuations σ_v shown in Fig. 4.3(b) undergo a rapid increase. We will discuss this feature afterwards.

Upon further increasing the amplitude of driving, $a > 1.5$, the Brownian motor generates a directed transport behavior. We also observe that the corresponding width of the weakly asymmetric, time averaged asymptotic velocity distribution $P_{as}(v)$ slightly decreases (see the first column on Fig. 4.5), meaning that the velocity fluctuations become smaller. The following explanation thus applies: Because at $a < 1.5$ escape jumps between the neighboring wells are rare, i.e., the average directed current is very small (note also the accompanying, very weak asymmetry in the distribution $P_{as}(v)$ shown in the first row in the Fig 4.5 for $a = 0.68$). The input energy is pumped primarily into the kinetic energy of the intra-well motion and

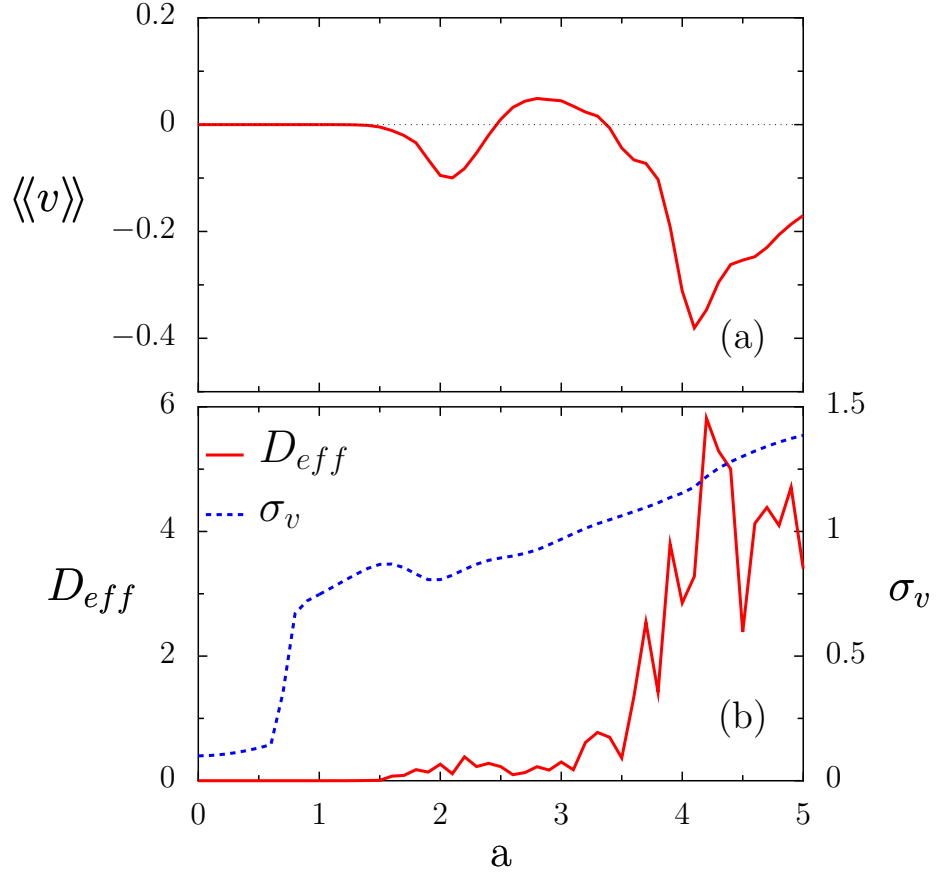


Figure 4.3: Fluctuation behavior of an inertial Brownian motor versus the driving strength a . Upper plot (a): averaged dimensionless velocity $\langle\langle v \rangle\rangle$ of the inertial Brownian motor in Eq. (2.4). Bottom plot (b): variance of the corresponding velocity fluctuations σ_v and effective diffusion D_{eff} . All quantities have been computed for the rescaled ratchet potential depicted on Fig. 2.2(b) and defined in eq. (2.19) with the parameter set (b) (see section [2.2] for details). The force corresponding to this potential ranges from $a_{c1} = -2.14$ to $a_{c2} = 4.28$. The angular frequencies at the well-bottom and at the barrier-top, respectively, equal each other, reading 5.28. The remaining rescaled parameters read: friction $\gamma = 0.5$, angular driving frequency $\omega = 3.6$ and weak thermal noise of strength $D_0 = 0.01$.

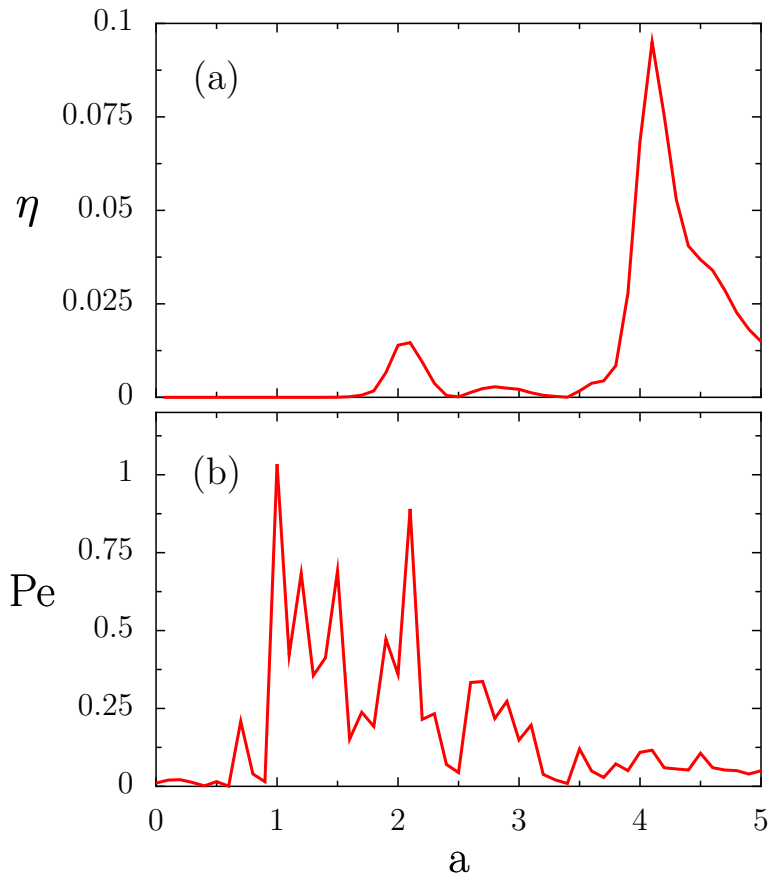


Figure 4.4: Dimensionless factors describing the performance of the Brownian motor depicted versus the driving strength a . Upper plot (a): rectification efficiency (or Stokes efficiency) defined in Eq. (3.6). Bottom plot (b): the Péclet number defined in (3.2). Rescaled parameters and the ratchet profile are the same as in the Fig. 4.3.

eventually is dissipated. As a is increased further, the Brownian motor mechanism starts to work, and some part of energy contributes to the net motion of the particle. Therefore, less energy remains available to drive intra-well oscillations and consequently the distribution $P_{as}(v)$ shrinks and the motor optimizes its performance. Above the upper threshold value of the potential force $a_{c2} \simeq 4.28$ the current starts to decrease because of the weakened influence of the ratchet potential at large rocking amplitudes.

The occurrence of multiple reversals of the directed current, as it is depicted in Fig. 4.3 (a), is a known, interesting feature of inertial Brownian motors. Several prior studies did elucidate in greater detail the corresponding mechanism [77, 103, 104, 107–113]. Here, we take instead a closer look at the current fluctuations and the effective diffusion. We observe that for the chosen set of parameters the maximal absolute stationary velocity on the Fig. 4.3 (a) does not exceed the value 0.4. In contrast, its fluctuations keep growing as the driving amplitude rises mostly due to the complicated way of motion – see the 2nd column on the Fig 4.5. Generally beside the usual transitions consistent with the mean velocity the particle sometimes goes in the opposite direction and performs intra-well oscillations. At large driving, the particle hardly feels the potential and undergoes a rocked, almost free Brownian motion with velocity fluctuations growing proportional to a , cf. the dashed line in the Fig. 4.3 (b). Within this directed transport regime, the rectification efficiency (3.6) and the equivalent Stokes efficiency (3.5) remain rather small, cf. the Fig. 4.4 (a). Such small rectification efficiency is the rule for this driven inertial Brownian motor.

For the small driving, with almost no transitions present, it is clear that the effective diffusion almost vanishes. When the motor starts to transport ($a \simeq 1.5$) the Brownian particles gain enough energy to cross the potential barrier, but due to the undirected thermal forces, they spread out as time goes by. The effective diffusion starts to grow as we increase the driving strength. For the highest $\langle\langle v \rangle\rangle$ we notice that the diffusion gets suppressed reflecting the more regular motion of the particles, which now proceed in a more coherent manner, cf. the third column on the Fig 4.5 for $a = 4.1$.

Moreover, one can observe two current reversals on the Fig. 4.3 (a), so there are two additional points where average velocity equals zero, but we perceive no corresponding vanishing of the effective diffusion. It means that there are still transitions present in the system for this driving strengths. The mean velocity equals zero according to the fact that the number of jumps to the right and to the left are equal.

The above described behavior has its reflection in a Péclet number cf. the Fig. 4.4 (b). Its maximal value for the generic driving parameters is found of about $Pe \simeq 1$. It indicates the typical high relative randomness of the transport, i.e. the highly diffusive motion of the particles. The best performance is not surprisingly found for the largest value of the velocity and corresponding largest values of Pe and η_R .

Let us next inspect the distribution $P_{as}(v)$ shown on the first column of the Fig. 4.5. These probabilities look rather symmetric; however, a finite ratchet velocity requires a certain amount of asymmetry either in the location or the width of the velocity peaks. Here, the current results mainly due to a slight shift of the maxima location.

The most peculiar feature of the current distributions shown in the first column of Fig. 4.5

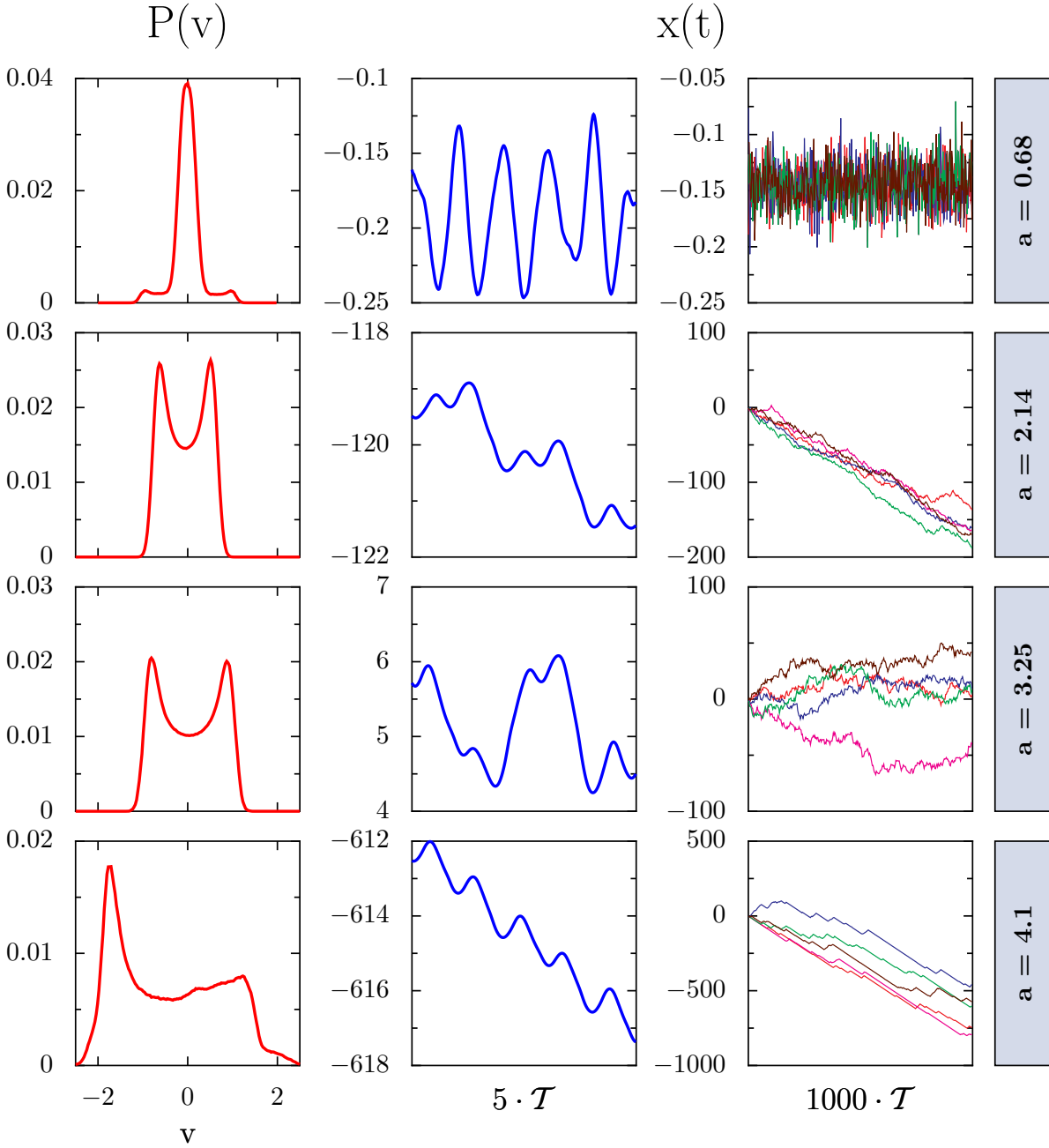


Figure 4.5: Time averaged asymptotic velocity distributions (1st column), short-time trajectories of $5\mathcal{T}$ (2nd column) and long-time trajectories of $1000\mathcal{T}$ (3rd column) plotted for the selected driving amplitudes, i.e. $a = 0.68, 2.14, 3.25, 4.1$. The remaining rescaled parameters read: friction $\gamma = 0.5$, angular driving frequency $\omega = 3.6$ and weak thermal noise of strength $D_0 = 0.01$.

is the emergence of two additional side-peaks for $a \gtrsim 0.6$ centered near $v = \pm 1$, which eventually dominate $P_{as}(v)$ at larger driving amplitudes. Of course, for zero drive we recover the strictly symmetric single-peaked Maxwell distribution, with the maximum at $v = 0$.

What is the origin of those three peaks in the distribution $P_{as}(v)$? Our first conjecture to connect it with the 'running' solutions turned out to be incorrect. This is so, because for $a \lesssim 1$ the particle rarely leaves the confining potential well and thus cannot significantly contribute to the side peaks of the distribution function. Further, we checked the outcome for the distribution $P_{as}(v)$ when reflecting barriers were placed at the maxima of the potential. Under such constraints, the three-peak-structure is recovered as well. Moreover, the sinusoidally driven damped particle in a harmonic potential can exhibit both, a singly-peaked as well as a double-peaked averaged velocity distribution [118]. However, for the parabolic potential that fits best the wells of our ratchet potential around its minima, we found a single peaked $P_{as}(v)$.

We therefore do conclude that the characteristic behavior for the additional side-peaks is rooted in the nonlinear, anharmonic character of the corresponding well of the periodic asymmetric ratchet profile.

4.1.3 Noisy dynamics: Fluctuations versus noise strength

In the Fig. 4.6, we present the results of the numerical analysis of the directed transport versus the rescaled temperature D_0 . We chose a sub-threshold driving strength for which the thermal noise plays a constructive role by inducing noise activated jumps across the potential barriers. We set $a = 0.8$ and the other parameters remain the same as in the previous section. In the Figures 4.6 and 4.7 we have plotted the calculated quantifiers as a function of rescaled temperature D_0 in the range from small rescaled temperature $D_0 = 0.01$ up to the thermal energy comparable with the barrier height ΔV of the ratchet potential (i.e. $D_0 = \Delta V = 1$). A further increase of temperature suppress the influence of the asymmetric ratchet potential and, consequently, the directed transport degrades.

Moreover, the time-averaged velocity distribution depicted in the first column of the Fig. 4.8 approaches the equilibrium velocity distribution as we increase temperature. For small D_0 the movement is typically bounded to oscillations inside the well of the ratchet potential with accompanying very rare transitions. For the high temperatures all the characteristics reflects the highly random motion, see also the third column of Fig. 4.8. A shallow, local minimum occurs for the velocity fluctuations, cf. dashed line in Fig. 4.6 (b) where the average current itself is maximal. These fluctuations are, however, notably three orders of magnitude *larger* than the directed current. Accordingly the rectification efficiency shown in Fig. 4.7 (a) is quite small.

The effective diffusion (solid line on the Fig. 4.6 (b)) exhibits rather large values and the corresponding Péclet number (see Fig. 4.7 (b)) has therefore small values. At any temperature, for a small driving amplitude a , the particle possesses very small efficiency and act in a rather random manner performing rare transitions. The spatial spreading over the wells of the ratchet potential is therefore large. Again, the Brownian motor is not operating efficiently.

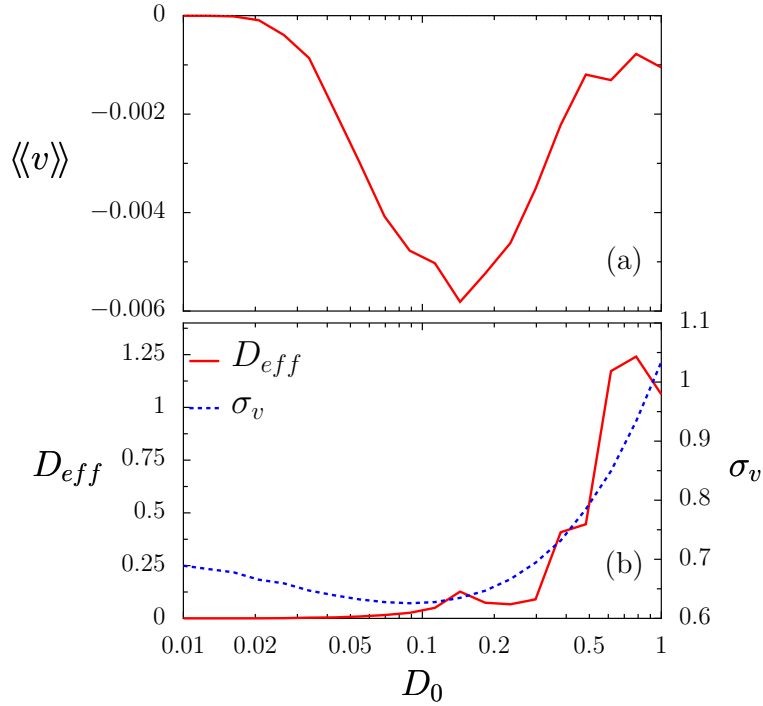


Figure 4.6: Fluctuation behavior of an inertial Brownian motor versus the noise strength D_0 . Upper plot (a): averaged dimensionless velocity $\langle\langle v \rangle\rangle$ of the inertial Brownian motor in Eq. (2.4). Bottom plot (b): variance of the corresponding velocity fluctuations σ_v and effective diffusion D_{eff} . All quantities have been computed for the rescaled ratchet potential depicted on Fig. 2.2(b) and defined in eq. (2.19) with the parameter set (b) (see section [2.2] for details). The angular frequencies at the well-bottom and at the barrier-top, respectively, equal each other, reading 5.28. The remaining rescaled parameters read: friction $\gamma = 0.5$, angular driving frequency $\omega = 3.6$ and weak driving strength $a = 0.8$.

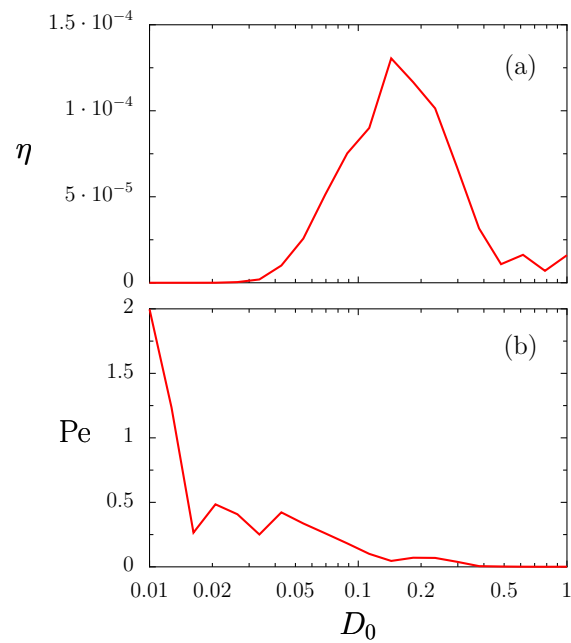


Figure 4.7: Dimensionless factors describing the performance of the Brownian motor depicted versus the rescaled temperature D_0 . Upper plot (a): rectification efficiency (or Stokes efficiency) defined in Eq. (3.6). Bottom plot (b): the Péclet number defined in (3.2). Rescaled parameters and the ratchet profile are the same as in the Fig. 4.6.

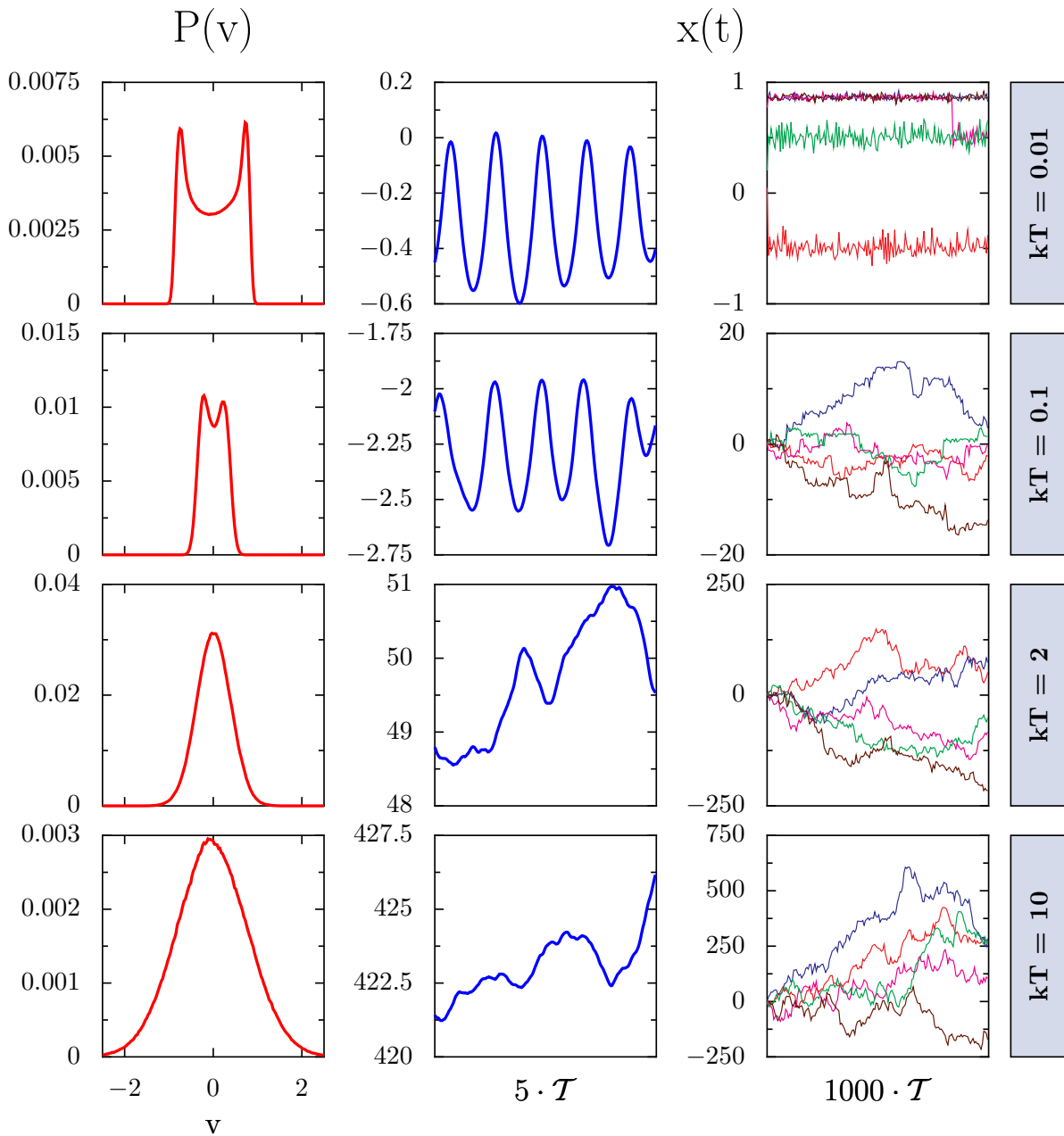


Figure 4.8: Time averaged asymptotic velocity distributions (1st column), short-time trajectories of $5\mathcal{T}$ (2nd column) and long-time trajectories of $1000\mathcal{T}$ (3rd column) plotted for the for selected noise strengths, i.e. $D_0 = 0.01, 0.1, 2, 10$. The remaining rescaled parameters are the same as on Fig 4.6.

4.2 Optimization of the performance

Thus far, changing the temperature of the ratchet environment or the driving strength did not lead to a large enhancement of the rectification efficiency. What is needed in achieving a large rectification efficiency is a sizable Brownian motor current which is accompanied by small current fluctuations, see Eq. (3.6). It is also highly desirable to have a small spatial spreading of the realizations of the process described by the Langevin equation (2.4). This scenario seemingly implies that the Brownian particles should proceed in a persistent manner with very few, occasional back-turns only. This in turn causes small fluctuations in the velocity and, additionally, provides a dominating asymmetry of the time averaged asymptotic velocity distribution.

Such a behavior can be realized by a combined tailoring of the asymmetry of the ratchet potential together with the use of appropriate driving conditions. In the quest for achieving such a favorable situation we use the three-harmonics ratchet potential plotted in the Fig. 2.2 for the set (c). Our hope is that upon minimizing the noise further we can achieve a substantial improvement of the efficiency.

At *very weak noise* and large, nonadiabatic rocking frequencies, this inertial Brownian motor starts moving efficiently for the values of the driving strength of about $a = 3.7$, see Fig. 4.9 (a). Because the directed velocity becomes maximal and simultaneously the fluctuations in both position and velocity space are locally minimal, see in Fig. 4.9 (b), we indeed find the desired enhancement of the rectification efficiency, see Fig. 4.10 (a).

We have studied several other ratchet potentials by varying the parameters c_1 and c_2 in Eq. (2.19) and still found regimes where the inertial ratchet works with a high efficiency (not shown). In all these cases we found that the velocity distribution has a support concentrated mainly on one of the semi-axes. Strongly asymmetric velocity distributions are depicted in the first column of Fig. 4.11. In contrast, with the mode c_2 set zero (see in Fig. 2.2 (b)) we could not identify such an optimal regime for the rectification of noise. The shape of these distributions just corroborates the fact that large rectification efficiencies are the result of persistent, (uni)-directional Brownian motor motion, accompanied by a strong asymmetry of the current statistics, see Fig. 4.11.

Let's take a closer look at the trajectories of the optimally working ratchet. Typically, there are two possible dynamical states of the ratchet system: a locked state, in which the particle oscillates mostly within one potential well (cf. the case with amplitude $a < 3$ or e.g. $a = 4.73$ in Fig. 4.11), and a running state, in which the particles surmount the barriers of the potential. Moreover, one can distinguish two classes of running states: either the particle overcomes the barriers without any back-turns (stable running states – cf. the case with an amplitude $a = 3.70$ in Fig. 4.11) or it undergoes frequent oscillations and back-scattering events (unstable running states – cf. the case with amplitude $a = 3.37$ in Fig. 4.11). For a small driving amplitude, we find that the locked behavior is generic implying that the average motor velocity is almost zero, see Fig. 4.11. If the amplitude is increased up to some critical value, here $a \simeq 3.25$, the running solutions emerge. About this critical point, for $a = 3.37$, the particle alternates between running and locked states, and uses energy for both barrier crossings and intra-well

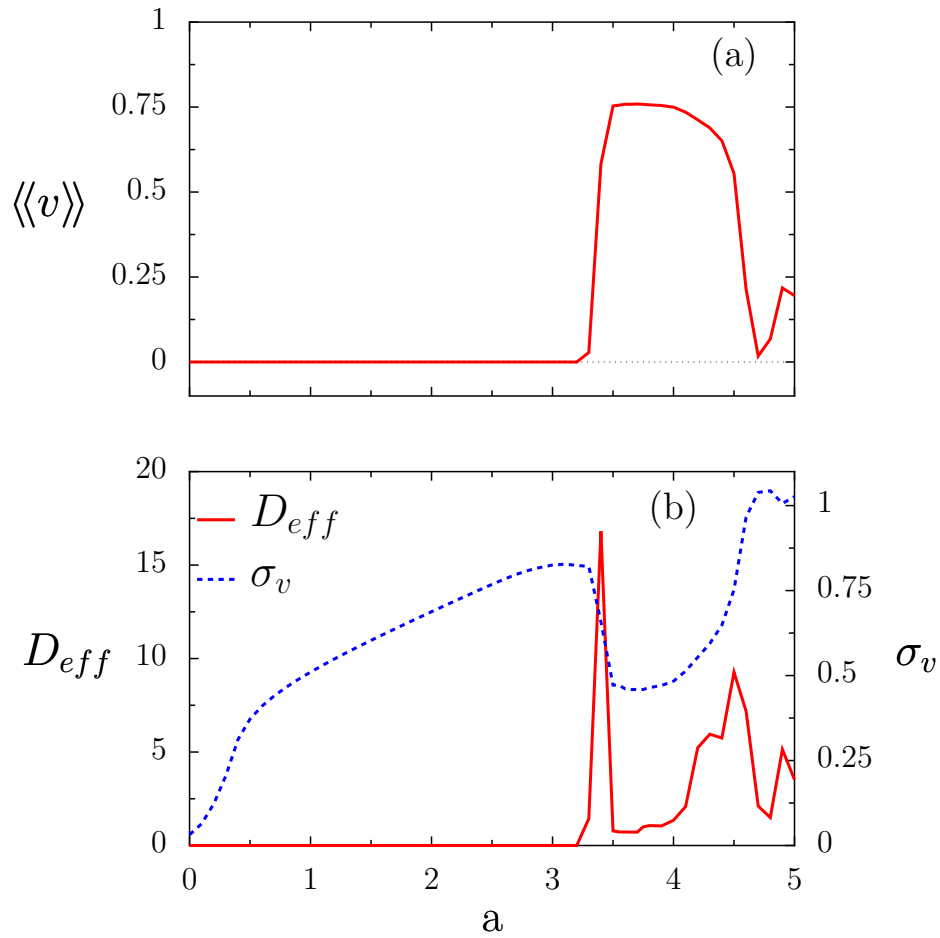


Figure 4.9: Top: the average, dimensionless velocity $\langle\langle v \rangle\rangle$ of the inertial, rocked Brownian motor under nonadiabatic driving conditions. Bottom: corresponding velocity fluctuations σ_v (dotted line) and corresponding diffusion coefficient D_{eff} (solid line). Values of the remaining parameters are the same as in Fig. 4.11.

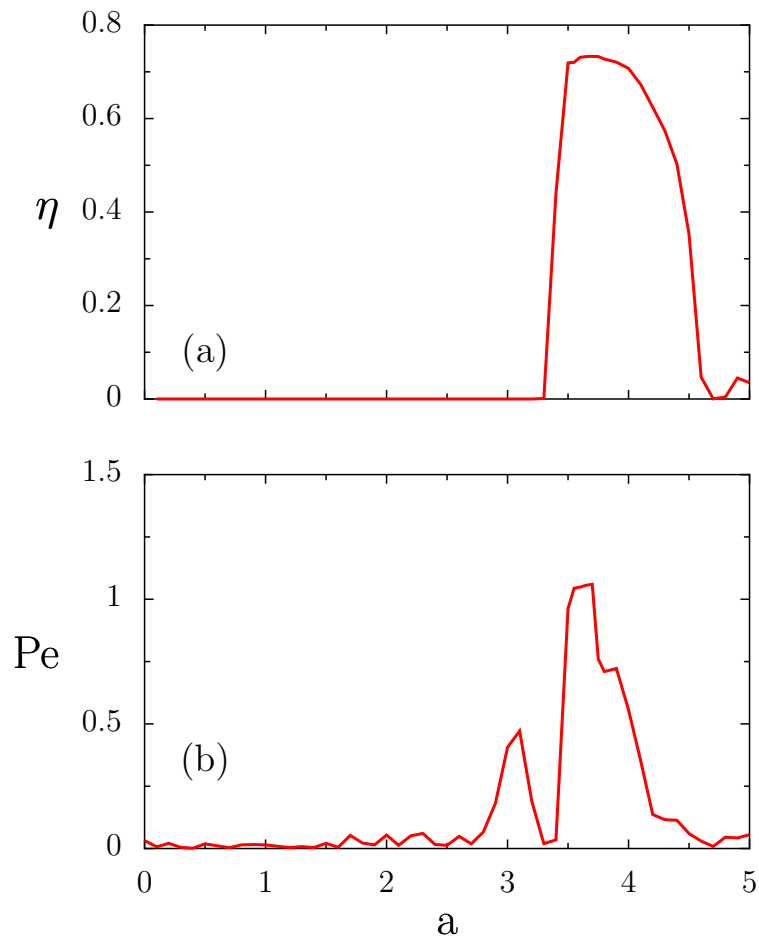


Figure 4.10: Top: Brownian motor efficiency η . Bottom: depicted is the Péclet number Pe , being proportional the inverse of the Fano factor. All quantities are plotted versus the external driving amplitude a . Values of the remaining parameters are the same as in Fig. 4.11.

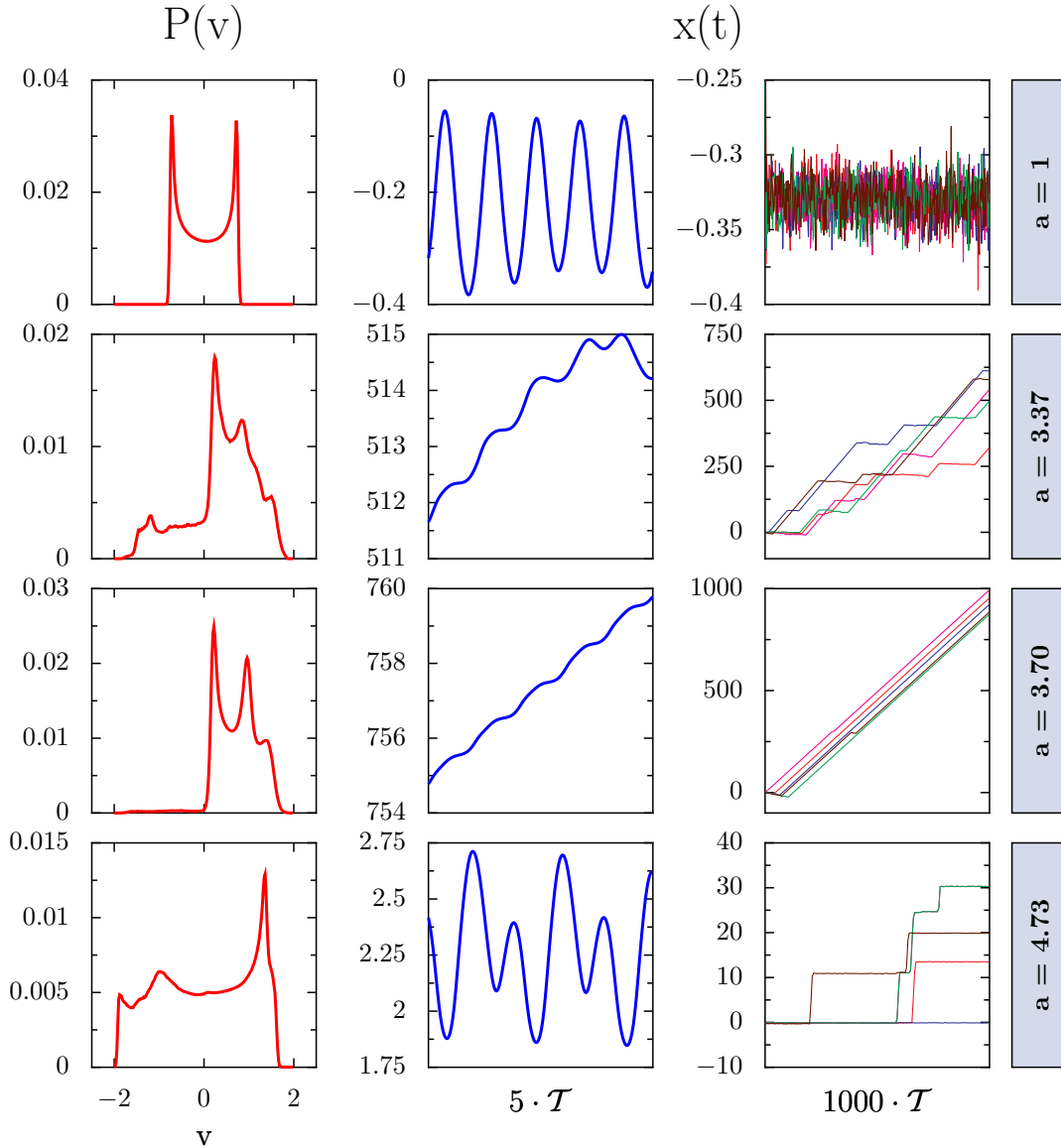


Figure 4.11: Time averaged asymptotic velocity distributions (1st column), short-time trajectories of $5\mathcal{T}$ (2nd column) and long-time trajectories of $1000\mathcal{T}$ (3rd column) of the rocked particle moving in the asymmetric ratchet potential shown on Fig. 2.2 (c). The forces stemming from such a potential range between -4.67 and 1.83 . The two angular frequencies at the well-bottom and at the barrier-top are the same, reading 5.34 . The remaining parameters are: $\gamma = 0.9$, $\omega = 4.9$ and $D_0 = 0.001$. One can see that for $a = 1$ and 4.73 the particles usually oscillate in a potential well, most of the time performing none or only a few steps. This results in an almost zero mean velocity, a very small effective diffusion but with rather large velocity fluctuations. For another set of driving amplitudes: $a = 3.37$ the mean velocity is large, σ_v becomes suppressed, but the effective diffusion exhibits an enlargement due to a “battle between attractors”. The case $a = 3.70$ corresponds to the optimal *modus operandi* of the inertial Brownian motor - the net drift is maximal and fluctuations are suppressed.

oscillations (see the second row in Fig. 4.11). This behavior is reflected in an enormous enhancement of the effective diffusion [65, 83, 119–121].

If the driving amplitude is further increased, a regime of optimal transport sets in. The rapid growth of the average velocity is accompanied by a decline of both the position and the velocity fluctuations. It means that the different realizations of the process (2.4) stay closely together; note the case $a = 3.70$ in Fig. 4.11. Because there are no intra-well oscillations, the energy that is dissipated per unit distance, is minimal.

At even larger drive amplitudes an upper threshold is approached, where the velocity sharply decreases to a value close to zero. Moreover, the diffusion coefficient is small and the velocity fluctuations are large, cf. the case with amplitude $a = 4.73$ in the Fig. 4.11. In this regime, the particle dangles around its actual position, as it occurs for $a < 3$, meaning that its motion is confined mostly to one well. We note, however, that the amplitude of the intra-well oscillations becomes much larger so that the corresponding velocity fluctuations are also large.

We conclude that the diffusion coefficient is small for cases when the particle performs either locked motion or stable running motion.

All these considerations are accurately encoded and described by the two previously discussed measures, namely, the efficiency η (3.6) and the Péclet number Pe in (3.2). It is found that the optimal regime for the ideal modus operandi of the Brownian motor is achieved when both the efficiency and the Péclet number become maximal, see in Fig. 4.10. Indeed, in this regime of optimal performance, the particle moves forward steadily, undergoing rare back-turns [105], see the case $a = 3.70$ in the Figures 4.11 – 4.10.

5 Inertial motor under load

We explore now how an external static load force influences the driven noisy dynamics 2.4. In particular this chapter treats the behavior of the noise-activated, directed current of an inertial Brownian motor as a function of an external bias, thus yielding the velocity-load behavior and performance in presence of an external conservative load force when inertial effects dominate. Varying the load force from negative to positive values the current of the inertial Brownian particle goes through zero at what is defined as the stall force F_{stall} . If the particle moves with a positive mean velocity for negative load forces, than for the interval $F \in [F_{stall}, 0]$ the particle does work against the external load.

We will demonstrate that a rocked, inertial Brownian particle, if put to work against a load, can exhibit *negative differential mobility* [122] and even *absolute negative mobility* [123] i.e. that the current decreases with increasing force or that the particle moves in the opposite direction of the force, respectively. This extraordinary phenomenon has been observed within a quantum mechanical setting for electron transfer phenomena [124], for ac-dc-driven tunnelling transport [125], in the dynamics of cooperative Brownian motors [126–128], Brownian transport with complex topology (entropic ratchets) [129–134] and in some stylized, multistate models with state-dependent noise [135, 136], to name but a few.

5.1 Biasing the ratchet

5.1.1 Current-load behavior and negative differential mobility

The complex inertial Brownian evolution can manifest its counterintuitive nature when we test its response to a constant external load force. In Fig. 5.1 we depict the load-velocity characteristics of a particular Brownian motor (2.4). Contrary to the familiar, monotonic dependence found for overdamped ratchet dynamics [73, 137], the velocity-load-behavior becomes now considerably more complex, exhibiting distinct non-monotonic characteristics. Around the forces $F \simeq -1.4$ and $F \simeq 0$ an increase of the bias F results in a corresponding decrease of the average velocity. This behavior is termed *negative differential mobility*. The effect is extremely pronounced for small positive load forces.

Let us elucidate the underlying working mechanism in greater detail: For the parameter values specified as in Fig. 5.1, at zero load the corresponding deterministic dynamics possesses a single stable attractor of period one which translocates the particle to the neighboring ratchet potential well during one period \mathcal{T} of driving (see the section 4.2)

$$\begin{aligned}x(t + \mathcal{T}) &= x(t) + 1, \\v(t + \mathcal{T}) &= v(t).\end{aligned}\tag{5.1}$$

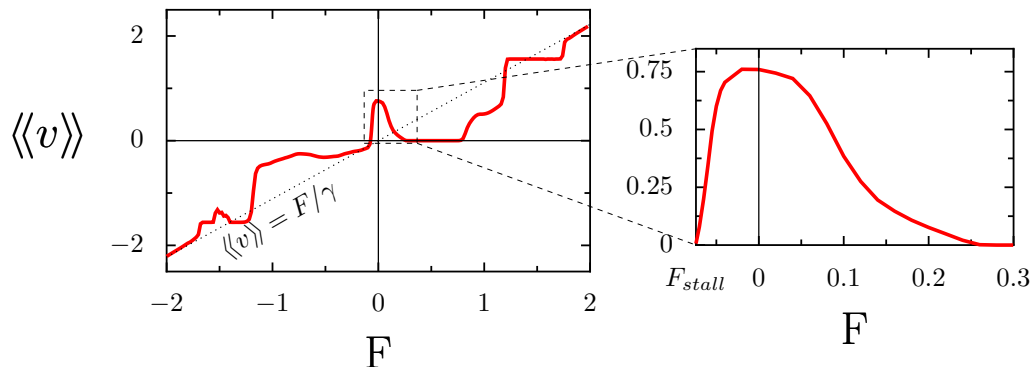


Figure 5.1: Average velocity of the inertial Brownian motor (2.4) as a function of an external, constant force F . The system parameters are: $a = 3.7$, $\omega = 4.9$, $\gamma = 0.9$ and $D = 0.001$. The dotted line denotes the average velocity of a particle moving in the absence of a periodic potential, being the limiting case for the Brownian motor dynamics at $F \rightarrow \infty$. One can notice a few regimes where the differential mobility ($\partial\langle\langle v \rangle\rangle/\partial F$) assumes a negative value. The most pronounced such behavior occurs for small positive values of the bias F (depicted in the inset). For bias forces $F \in (F_{stall}, 0)$, $F_{stall} \simeq -0.074$, the Brownian motor performs against the external load.

In the presence of weak noise, this periodic motion is robust in the sense that the eq. (5.1) still holds in distribution. The particle moves with a high Stokes efficiency as a consequence of small fluctuations of the velocity from its average value. To realize this periodic regime, however, requires that all system parameters are precisely tuned. Any small external load F , regardless of its sign, drives the system away from this most efficient regime and the average velocity starts dropping to smaller values. In particular a small positive force leads to a decrease of the average velocity and consequently to a negative differential mobility. In contrast, at very large magnitudes of the load force F , the periodic potential force becomes less important and the velocity eventually assumes its asymptotic value, reading $\langle v \rangle = F/\gamma$.

5.1.2 Efficiency of forced and rocked Brownian motors at optimal driving conditions

As we remarked already above with the parameters of Fig 5.1, the Brownian motor operates optimally near the bias $F \simeq 0$. With Fig. 5.2 (a), we depict the behavior of the Stokes efficiency within an interval of bias forces $F \in (F_{stall}, 0)$ where the motor does work against the external force. The Stokes efficiency assumes a value of about 0.75 at $F = 0$, and monotonically decreases with decreasing load, reaching zero at the stall force $F_{stall} \simeq -0.074$, where the average velocity vanishes. For loads within the interval $(F_{stall}, 0)$, the ratchet device pumps particles against the bias, cf. Fig. 5.1. The behavior of the rectification efficiency in this regime closely matches the behavior of the Stokes efficiency. Indeed, within this forcing

regime the efficiency of energy transduction η_E assumes much smaller values than the Stokes efficiency η_S , see Fig. 5.2 (b). Within this forcing regime the bell-shaped character of η_E is an immediate consequence of its definition in eq. (3.4): It acquires vanishing values at the stall force, where the velocity becomes zero and at $F = 0$, where the output power vanishes. In between the average input power P_{in} varies only slightly.

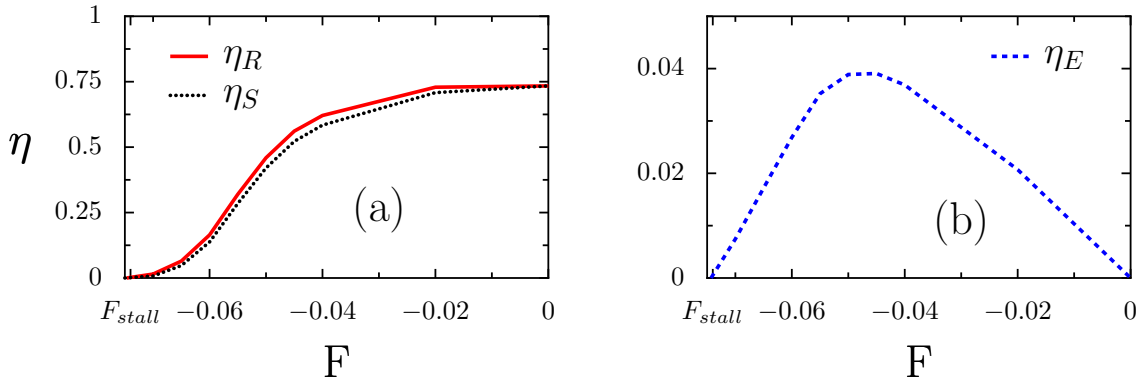


Figure 5.2: Behavior of different efficiency measures within the regime of "uphill motion". Depicted are the efficiency of rectification η_R , the closely related Stokes efficiency η_S , in panel (a), and the efficiency of energy conversion η_E , panel (b), versus the external load F , varying between the stall force F_{stall} and the vanishing bias $F = 0$. The Stokes efficiency assumes much larger values than the corresponding energetic one; it is therefore dominating the viscous, noise-assisted transport. The driving parameters are the same as in Fig. 5.1.

5.2 Absolute negative mobility in a symmetric potential

In the following the influence of noise and load on the motion of the particle in a symmetric sinus potential is addressed

$$V(x) = \sin(2\pi x). \quad (5.2)$$

It is obvious that for a zero tilt and a symmetric potential one cannot produce any directed motion in the system. If we tilt the system, we break the symmetry and net motion appears, usually in the direction given by the tilt. Sometimes, however, the dynamics turns out to be very counterintuitive.

In this section we set the system parameters as follows: the strength of the external driving $a = 4.2$ with the angular frequency $\omega = 4.9$, the friction $\gamma = 0.9$ and the low temperature $D_0 = 0.001$. We can identify the stall forces as $F_{stall}^{\pm} \simeq \pm 0.17$. For strong loads the average velocity is not much different from that of a free particle i.e. $\langle\langle v \rangle\rangle = F/\gamma$. It means that the particle does not feel the potential anymore, and slides down more or less freely.

The solid line on the Fig. 5.3 corresponds to the current – load plot for the Brownian particle in a symmetric sinus potential. One can notice that for a small load forces the Brownian parti-

cles move against the force. This behavior is called *absolute negative mobility*. This stunning behavior is a purely noise-induced feature. In the range of load force between $[F_{stall}^-, F_{stall}^+]$, for a deterministic part of equation 2.4 (see the dashed line in the Fig. 5.3) the particle dwells in one place resulting in a zero net motion.

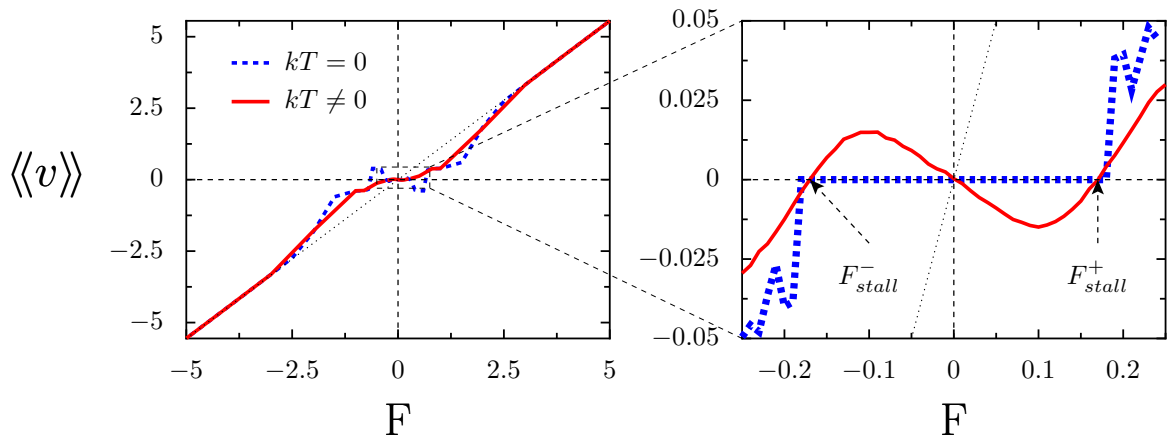


Figure 5.3: Average velocity of the inertial Brownian particle in a symmetric sinus potential (2.19 a) depicted as a function of an external, constant force F for the deterministic (dashed line) and noisy (solid line) dynamics. The system parameters are: $a = 4.2$, $\omega = 4.9$, $\gamma = 0.9$ and $D = 0.001$. The dotted line denotes the average velocity of a particle moving in the absence of a periodic potential, being the limiting case for the Brownian motor dynamics at $F \rightarrow \infty$. The most prominent regime where the absolute mobility ($\langle\langle v \rangle\rangle/F$) assumes a negative value is shown in the center plot. The most pronounced such behavior occurs for small absolute values of the bias F . For bias forces $F \in [F_{stall}^-, F_{stall}^+]$ with $F_{stall}^\pm \simeq \pm 0.17$, the Brownian particle performs against the external load.

Although this feature is purely noise induced, it still has, its roots in the deterministic structure of attractors. The situation is completely symmetric with respect to $F = 0$, so we will focus on the small positive load $F = 0.1$. For a given driving strength $a = 4.2$ there exists one stable attractor, which causes the particle to dwell in one potential well according to the external periodic driving, see first column in Fig. 5.4. If we, however, heat up the system a bit, the thermal random force kicks out the particle from the stable attractor, and impose the dynamics to relax again and again. The structure of the deterministic phase space for small times (including the transient effects) is shown in the second column in Fig. 5.4. It means that with noise the particle is able to proceed with a negative velocity while in a deterministic case, after relaxation, it stays in a locked state forever. For a noisy dynamics we can see this situation as the ghost attractors of a negative direction on a phase space, see Fig. 5.5. Both situations, deterministic with transient effects and noisy, give almost the same picture of the phase space, c.f. second column in Fig. 5.4 and Fig. 5.5.

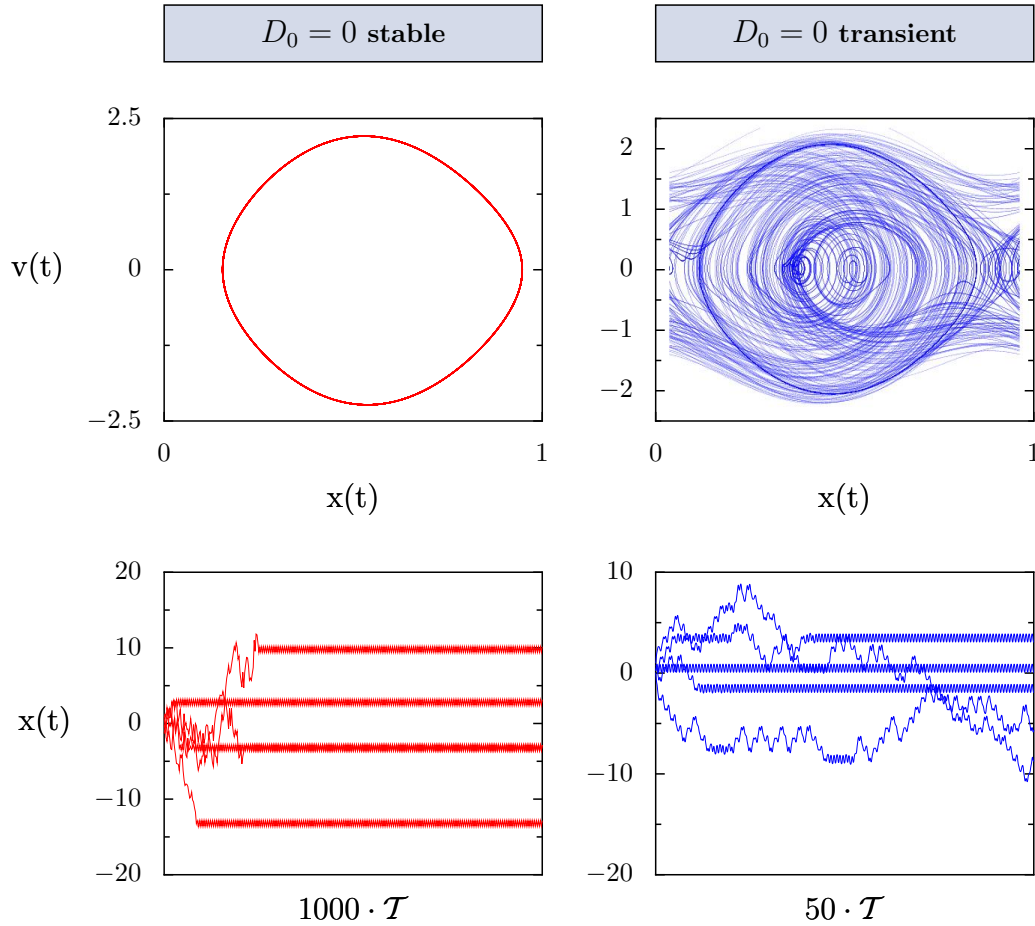


Figure 5.4: Deterministic motion shown for the parameters: $\gamma = 0.9$, $\omega = 4.9$, $F = 0.1$ and $a = 4.2$. We took uniformly distributed initial conditions in ranges $x_0 \in [0, 1]$ and $v_0 \in [-0.2, 0.2]$.

Upper row: The phase space (instantaneous velocity versus position). On the left we show period one locked attractor that produces zero current. On the right we show the transient effects, resulting in a very complicated picture of the phase space.

Lower row: Trajectories of the particles shown as an illustration of the attractors plotted in the upper row. To show transient effects in more details we used only 50 periods \mathcal{T} long runs of the deterministic motion.

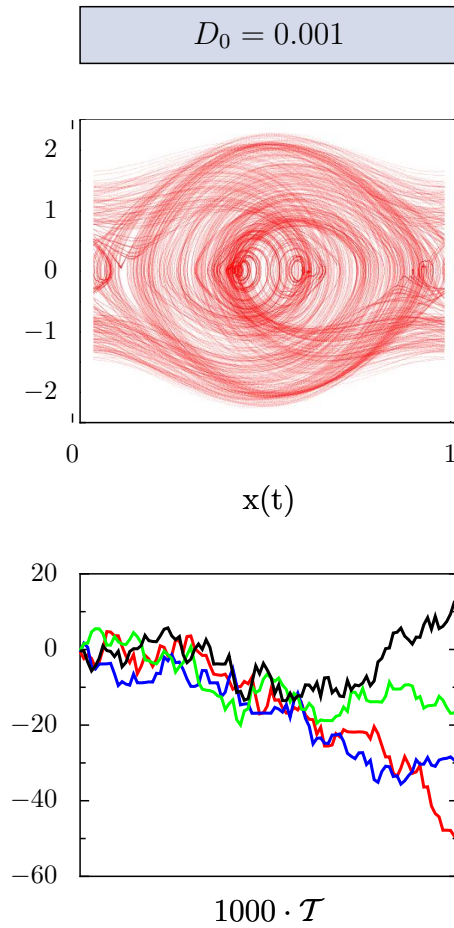


Figure 5.5: Stochastic motion shown for the parameters: $D_0 = 0.001$, $\gamma = 0.9$, $\omega = 4.9$, $F = 0.1$ and the driving strength $a = 4.2$. Upper plot: The phase space (instantaneous velocity versus position). Lower plot: Stochastic trajectories of the particle moving in a tilted rocked sinus potential.

We now take a look at the efficiency of the Brownian particle in the periodic symmetric potential under influence of the the load force. As already said zero bias means zero current resulting in the zero efficiency. For a non vanishing bias we can determine the efficiencies defined in the section 3.2. In the Fig. 5.6 we showed the relative amount of work done against all forces together (solid line) and also against the load and viscous forces separately (the dashed and dotted line, respectively). We notice that all three efficiencies are very small compared to the optimally working ratchet, with maximal values of the order of 10^{-3} . The weakest effect is found for the Stokes efficiency η_S . It means that almost all average output power is used for a motion against the load, cf. the efficiency of the energy conversion η_E (the dashed line in Fig 5.6). It is a completely different situation of what we have found for a ratchet potential with the optimal driving conditions, presented in the previous section. The work done by the Brownian motor against the load was very small and the particle struggles mostly against the Stokes force.

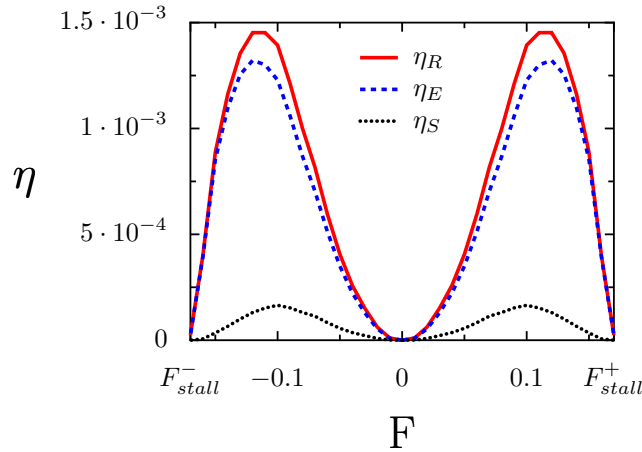


Figure 5.6: Different efficiencies measures as defined in section 3.2, of the inertial Brownian particle in a symmetric sinus potential (2.19 a) plotted as a function of an external, constant force $F \in [F_{stall}^-, F_{stall}^+]$. Note that the plotted curves are strictly symmetric with respect to $F = 0$. The system parameters the same as in the Fig. 5.3.

6 Summary and Conclusions

In this thesis the properties of the transport of a *massive* Brownian particle moving in a periodic potential with and without spatial symmetry are addressed. The system is driven out of an equilibrium state by an external, time periodic force. The case with an additional constant bias force was also investigated.

Strongly nonlinear systems far from equilibrium driven inertial ratchets belong to the class of extremely complex and complicated issues. Our model implies a large, 7-dimensional, parameter space, which is made up of: friction γ , external driving strength a and frequency ω , load force F , noise strength D_0 and two constants c_1 and c_2 that define the potential shape. As a tool for the analysis of the above formulated problem the numerical simulation of the corresponding Langevin equation (2.4) was used. This method, however, requires a relatively long CPU time to estimate all of the relevant quantifiers. It is therefore not possible to systematically explore totality of the parameter space. In order to achieve a deeper understanding of the system, we elucidated the dynamics for a few representative points of the parameter space in greater detail. In the numerical analysis we kept friction γ , frequency ω and both potential constants c_1 , c_2 fixed. We used the driving strength a , temperature D_0 and load force F as control parameters.

For inertial ratchets two characteristic times, the period of the external driving force $\mathcal{T} = 2\pi/\omega$ and the rescaled Stokes time τ_L/τ_0 , are relevant. In this thesis both were chosen to be of the same order. Being more specific: in the section 4.1 the time period $\mathcal{T} = 2\pi/3.6 \simeq 1.745$ and the Langevin time $\tau_L/\tau_0 = 2$; in the section 4.2 $\mathcal{T} = 2\pi/4.9 \simeq 1.282$ and $\tau_L/\tau_0 \simeq 1.111$. It means that we do not neglect the influence neither of the external driving nor of the inertia of the particle. In fact we need both of them incorporating to enhance the transport properties.

In this work, criteria for the optimal transport of an inertial rocked ratchet were established by means of two relevant quantifiers: the efficiency η and the *Péclet number* Pe . We can define several different efficiency measures that reflect the forces that a particle has to work against. Here the forces are: average Stokes force $\gamma\langle\langle v \rangle\rangle$ and load F so we can define an adequate efficiency for each of them. We have therefore Stokes efficiency η_S and efficiency of energy conversion η_E , that describe how much energy is used to proceed against the respective force. The sum of these two defines the *rectification efficiency* η_R , that describes how much of total energy pumped into the system is effectively used. From the numerical analysis it follows that the most efficient and regular transport is obtained when Péclet number and rectification efficiency are simultaneously large.

Performance of Brownian Motors

For a generic ratchet presented in the section 4.1, in the considered regime of the control parameters, the efficiency of maximum 10% and relatively random manner of motion was

found. The potential parameters can be adjusted to obtain a potential form with relatively flat slopes, like the potential used in the section 4.2. For this particular profile the characteristics of the motion are greatly enhanced, resulting in a rectification efficiency of about 70% and relatively high Péclet number at the optimal driving strength. For this particular strength we inspected the influence of an external static load force. We found that for small loads, regardless of the sign, the velocity of the particle drops to zero when we increase the bias. The external load destroys therefore the regular and efficient ratchet dynamics. For small positive loads a negative differential mobility, (i.e. $\partial\langle v \rangle / \partial F < 0$) was found.

Absolute negative mobility

Next we investigated the response of a particle moving in a symmetric sinusoidal potential to a static load force. Here, we have found another intriguing interplay between the deterministic and noisy dynamics, revealing an absolute negative mobility ($\langle v \rangle / F < 0$). This feature appears to be completely noise induced, as for the deterministic motion the averaged velocity equals zero for small loads.

Conclusions

Though the physics of these systems has been extensively studied in many different aspects for 25 years, there are still new and interesting phenomena waiting to be discovered. Up to our knowledge there exist no analysis of *underdamped* noisy systems where the influence of the friction force can be neglected. There are several papers exploring the deterministic properties of Hamiltonian ratchets [138–140] in both classical and quantum regime. The influence of the heat bath and therefore of thermal noise on a dynamics of systems with a very weak dumping is definitely interesting and promising topic.

The possibility of revealing the phenomenon of the absolute negative mobility in ratchets is definitely an interesting problem. For the ratchets known and well understood feature are current reversals (i.e. the change of sign of the current for different values of control parameter). It is highly probable that one could find absolute negative mobility in these very points, where the current changes its sign.

A Effective Diffusion

In this thesis we have considered the effective diffusion coefficient, which is defined as

$$D_{eff} = \lim_{t \rightarrow \infty} \frac{\langle x^2(t) \rangle - \langle x(t) \rangle^2}{2t}, \quad (\text{A.1})$$

where the brackets $\langle \cdot \rangle$ denote an average over the initial conditions of position and velocity and over all realizations of the thermal noise. Another definition of the diffusion coefficient is given by the formula

$$D = \lim_{t \rightarrow \infty} \frac{\langle [\delta x(t) - \delta x(0)]^2 \rangle}{2t}, \quad (\text{A.2})$$

where $\delta x(t) = x(t) - \langle x(t) \rangle$. By inspection one finds

$$D_{eff} = D \quad (\text{A.3})$$

if

$$\lim_{t \rightarrow \infty} \frac{1}{t} \langle \delta x(t) \delta x(0) \rangle = 0. \quad (\text{A.4})$$

In our case, this term vanishes because of the presence of thermal noise and dissipation. More generally, $|\langle \delta x(t) \delta x(0) \rangle|$ may increase at most as $t^{1/2}$ if the diffusion coefficient D as defined in (A.2) is finite. Consequently, for such processes the equation (A.3) also holds.

We now show that the diffusion constant D is related to the auto-correlation function of the velocity via a Green-Kubo relation, in spite of the fact that the system is far from equilibrium. For a system with periodic driving, D takes the form

$$D = \int_0^\infty ds \bar{C}(s), \quad (\text{A.5})$$

where

$$\bar{C}(s) = \frac{1}{T} \int_0^T d\tau C_{as}(\tau, s) \quad (\text{A.6})$$

denotes the time average of the velocity correlation function $C_{as}(\tau, s)$ over one period $T = 2\pi/\omega$ of the driving and where

$$C_{as}(t, s) = \langle \delta v(t) \delta v(t + s) \rangle_{as} \quad (\text{A.7})$$

is the nonequilibrium asymptotic velocity-velocity correlation function. In the case of periodic driving, this function is periodic with respect to the first argument, i.e.,

$$C(t, s) = C(t + T, s). \quad (\text{A.8})$$

To show the Green-Kubo relation, we start from the expression $\dot{x}(t) = v(t)$ from which it follows that

$$\delta x(t) - \delta x(0) = \int_0^t ds \delta v(s). \quad (\text{A.9})$$

Therefore (A.2) takes the form

$$\begin{aligned} 2D &= \lim_{t \rightarrow \infty} \frac{1}{t} \int_0^t ds_1 \int_0^t ds_2 \langle \delta v(s_1) \delta v(s_2) \rangle \\ &= \lim_{t \rightarrow \infty} \frac{1}{t} \int_0^t ds_1 \int_0^t ds_2 C(s_2, s_1 - s_2), \end{aligned} \quad (\text{A.10})$$

where

$$C(t, s) = \langle \delta v(t) \delta v(t + s) \rangle. \quad (\text{A.11})$$

Changing the integration variables $(s_1, s_2) \rightarrow (s = s_1 - s_2, \tau = s_2)$ and exploiting the symmetry of the correlation function, $C(t, s) = C(t + s, -s)$, one obtains

$$\begin{aligned} D &= \lim_{t \rightarrow \infty} \frac{1}{t} \int_0^t ds \int_0^{t-s} d\tau C(\tau, s) \\ &= \lim_{t \rightarrow \infty} \frac{1}{t} \int_0^t ds \int_0^t d\tau C(\tau, s) - \lim_{t \rightarrow \infty} \frac{1}{t} \int_0^t ds \int_{t-s}^t d\tau C(\tau, s). \end{aligned} \quad (\text{A.12})$$

We assume that the diffusion coefficient is finite. Therefore the second term in the second line of (A.12) tends to zero as $t \rightarrow \infty$, so that

$$D = \int_0^\infty ds \lim_{t \rightarrow \infty} \frac{1}{t} \int_0^t d\tau C(\tau, s). \quad (\text{A.13})$$

For $t = K\mathcal{T}$, one splits the second integral into sum over subsequent periods,

$$\begin{aligned} \lim_{t \rightarrow \infty} \frac{1}{t} \int_0^t d\tau C(\tau, s) &= \lim_{K \rightarrow \infty} \frac{1}{K\mathcal{T}} \sum_{k=1}^K \int_{(k-1)\mathcal{T}}^{k\mathcal{T}} d\tau C(\tau, s) \\ &= \frac{1}{\mathcal{T}} \int_0^{\mathcal{T}} d\tau C_{as}(\tau, s) = \overline{C}(s) \end{aligned} \quad (\text{A.14})$$

where

$$C_{as}(\tau, s) = \lim_{K \rightarrow \infty} \frac{1}{K} \sum_{k=0}^K C(\tau + k\mathcal{T}, s). \quad (\text{A.15})$$

The Eqs. (A.11), (A.13)-(A.15) represent the Green-Kubo relation for the diffusion constant of such periodically driven processes $x(t)$; notably, these *per se* constitute far from equilibrium processes.

B Efficiency

With this appendix we present the derivation of the expression (3.6) for the average input power. As already elaborated we combine the arguments in [79, 92, 96] and establish the efficiency η_R as in eq. (3.6)

$$\eta_R = \frac{\gamma \langle\langle v \rangle\rangle^2 + |F \langle\langle v \rangle\rangle|}{P_{in}}. \quad (\text{B.1})$$

In the denominator, P_{in} denotes the rate of the energy input to the system. To calculate P_{in} , let us recast (2.4) into the form

$$dx = v dt, \quad (\text{B.2})$$

$$dv = -\left(\gamma v + V'(x, t)\right) dt + \sqrt{2\gamma D_0} dW(t), \quad (\text{B.3})$$

where

$$V(x, t) = V(x) - ax \cos(\omega t) - Fx \quad (\text{B.4})$$

and $W(t)$ is the Wiener process

$$\langle W(t) \rangle = 0, \quad \langle W^2(t) \rangle = t. \quad (\text{B.5})$$

Now, we evaluate the ensemble and temporal averages of the re-scaled kinetic energy $G(v) = v^2/2$, $v = v(t)$. To this aim, first we apply Ito's differential calculus to the function $G(v)$ to obtain

$$d\left(v^2/2\right) = -\left(\gamma v^2 + vV'(x, t) - \gamma D_0\right) dt + \sqrt{2\gamma D_0} v dW(t). \quad (\text{B.6})$$

The ensemble average (i.e. the average over all realization of the Wiener process denoted by $\langle \cdot \rangle$) for the rate of change of the kinetic energy results in

$$\frac{d}{dt} \langle v^2/2 \rangle = -\left[\gamma \langle v^2 \rangle + \langle vV'(x) \rangle - \langle v a \cos(\omega t) \rangle - \langle Fv \rangle - \gamma D_0 \right],$$

where we exploited the (Ito)-martingale property (for the part containing the Wiener process). Next, we average over the temporal period as in (2.18) (periodic time-dependence of asymptotic probability). In doing so, we evaluate

$$\langle\langle \frac{d}{dt} v^2 \rangle\rangle = \frac{1}{\mathcal{T}} \left[\langle v^2(t + \mathcal{T}) \rangle - \langle v^2(t) \rangle \right] = 0. \quad (\text{B.7})$$

Likewise, for the contribution

$$\langle\langle vV'(x) \rangle\rangle = \frac{1}{\mathcal{T}} \left[\langle V(x(t + \mathcal{T})) \rangle - \langle V(x(t)) \rangle \right] = 0. \quad (\text{B.8})$$

Consequently, we obtain

$$0 = -\gamma \left[\langle\langle v^2 \rangle\rangle - D_0 \right] + F \langle\langle v \rangle\rangle + \langle\langle va \cos(\omega t) \rangle\rangle. \quad (\text{B.9})$$

We define the average input power as

$$P_{in} := |F \langle\langle v \rangle\rangle + \langle\langle va \cos(\omega t) \rangle\rangle|, \quad (\text{B.10})$$

i.e. the input energy to the system per unit time. From eq. (B.9) it follows

$$P_{in} = \gamma |\langle\langle v^2 \rangle\rangle - D_0|. \quad (\text{B.11})$$

Thus, upon combining (B.1) and (B.11) the relation for the rectification efficiency (3.6) emerges

$$\eta_R = \frac{\gamma \langle\langle v \rangle\rangle^2 + |F \langle\langle v \rangle\rangle|}{\gamma |\langle\langle v^2 \rangle\rangle - D_0|}. \quad (\text{B.12})$$

We also emphasize here, that our scheme for the efficiency of rectification at zero bias ($F = 0$) is *independent* of the transport friction-coefficient γ . This feature is in agreement with the corresponding result by Suzuki and Munakata [79].

Bibliography

- [1] R. Brown. A brief account of microscopical observations made in the months of June, July, and August, 1827, on the particles contained in the pollen of plants, and on the general existence of active molecules in organic and inorganic bodies. *Philos. Mag. N. S.*, 4:161, 1828.
- [2] R. Brown. Additional remarks on active molecules. *Philos. Mag. N. S.*, 6:161, 1829.
- [3] B. J. Ford. Brown's observations confirmed. *Nature*, 359:265, 1992.
- [4] A. Einstein. Über die von der molekularkinetischen Theorie der Wärme geforderte Bewegung von in ruhenden Flüssigkeiten suspendierten Teilchen. *Ann. Phys. (Leipzig)*, 17:549, 1905.
- [5] A. Einstein. Eine neue Bestimmung der Moleküldimensionen. *Ann. Phys. (Leipzig)*, 19:289, 1906.
- [6] W. Sutherland. A dynamical theory of diffusion for non-electrolytes and the molecular mass of albumin. *Philosophical Magazine*, 9:781, 1905.
- [7] M. Smoluchowski. Zur kinetischen Theorie der brownischen Molekularbewegung und der Suspensionen. *Ann. Phys.*, 21:756, 1906.
- [8] M. Smoluchowski. Drei Vorträge über Diffusion, brownische Molekularbewegung und Koagulation von Kolloidteilchen. *Physik. Zeitschr.*, 17:557–561 and 585–599, 1916.
- [9] L. Gouy. Note sur le mouvement brownien. *J. de Phys. Série 2*, 7:561, 1888.
- [10] J. Perrin. Les atomes. *Comptes Rendues Acad. Sci. Paris*, 158:1168, 1914.
- [11] M. Smoluchowski. Experimentell nachweisbare, der üblichen Thermodynamik widersprechende Molekularphänomene. *Physik. Zeitschr.*, 13:1069, 1912.
- [12] L. Gouy. Sur le mouvement brownien. *Comptes Rendues Acad. Sci., Paris*, 109:102, 1889.
- [13] R. P. Feynman, R. B. Leighton, and M. Sands. *The Feynman Lectures Of Physics*, volume 1. Addison Wesley, Reading, MA, 1963.
- [14] J.M.R. Parrondo and P. Espanol. Criticism of Feynman's analysis of the ratchet as an engine. *Am. J. Phys.*, 64:1125, 1996.

- [15] M. O. Magnasco and G. Stolovitzky. Feynman's ratchet and pawl. *J. Stat. Phys.*, 93:615, 1998.
- [16] J. Łuczka. Application of statistical mechanics to stochastic transport. *Physica A*, 274:200, 1999.
- [17] F. Jülicher, A. Ajdari, and J. Prost. Modeling molecular motors. *Rev. Mod. Phys.*, 69:1269, 1997.
- [18] P. Reimann. Brownian motors: Noisy transport far from equilibrium. *Phys. Rep.*, 361:57, 2002.
- [19] J. Łuczka, R. Bartussek, and P. Hänggi. White-noise-induced transport in periodic structures. *Europhys. Lett*, 31:431, 1995.
- [20] J. Prost, J. F. Chauwin, L. Peliti, and A. Ajdari. Asymmetric pumping of particles. *Phys. Rev. Lett.*, 72:2652, 1994.
- [21] R. D. Astumian and M. Bier. Fluctuation driven ratchets: Molecular motors. *Phys. Rev. Lett.*, 72:1766, 1994.
- [22] C. S. Peskin, G. B. Ermentrout, and G. F. Oster. *The correlation ratchet: A novel mechanism for generating directed motion by ATP hydrolysis*, page 479. Springer, New York, 1994.
- [23] J. Kula, T. Czernik, and J. Łuczka. Transport generated by dichotomous fluctuations. *Phys. Lett. A*, 214:14, 1996.
- [24] J. Kula, M. Kostur, and J. Łuczka. Brownian motion controlled by dichotomic and thermal fluctuations. *Chem. Phys*, 235:27, 1998.
- [25] I. Bena, M. Copelli, and C. Van den Broeck. Stokes' drift: A rocking ratchet. *J. Stat. Phys*, 101:415, 2000.
- [26] J. Luczka, T. Czernik, and P. Hänggi. Symmetric white noise can induce directed current in ratchets. *Phys. Rev. E.*, 56:3968, 1997.
- [27] M. Kostur, G. Knapczyk, and J. Luczka. Optimal transport and phase transition in dichotomic ratchets. *Physica A*, 325:69, 2003.
- [28] M. M. Millonas and M. I. Dykman. Transport and current reversal in stochastically driven transport. *Phys. Lett. A*, 185:65, 1994.
- [29] C. R. Doering, W. Horsthemke, and J. Riordan. Nonequilibrium fluctuation-induced transport. *Phys. Rev. Lett.*, 72:2984, 1994.

-
- [30] R. Bartussek, R. Reimann, and P. Hänggi. Precise precise numerics versus theory for correlation ratchets. *Phys. Rev. Lett.*, 76:1166, 1996.
- [31] P. Reimann, R. Bartussek, R. Häussler, and P. Hänggi. Brownian motors driven by temperature oscillations. *Phys. Lett. A*, 215:26, 1996.
- [32] M. Büttiker. Transport as a consequence of state-dependent diffusion. *Z. Phys. B*, 68:161, 1987.
- [33] Y. X. Li. Transport generated by fluctuating temperature. *Physica A*, 238:245, 1997.
- [34] Y. D. Bao. Directed current of Brownian ratchet randomly circulating between two thermal sources. *Physica A*, 273:286, 1999.
- [35] A. M. Jayannavar. Simple model for Maxwell's-demon-type information engine. *Phys. Rev. E.*, 53:2957, 1996.
- [36] P. Lancon, G. Batrouni, L. Lobry, and N. Ostrowsky. Drift without flux: Brownian walker with a space-dependent diffusion coefficient. *Europhys. Lett*, 54:28, 2001.
- [37] G. P. Harmer and D. Abbott. Parrondo's paradox. *Stat. Sci.*, 14:206, 1999.
- [38] G. P. Harmer and D. Abbott. Game theory: Losing strategies can win by Parrondo's paradox. *Nature*, 402:864, 1999.
- [39] J. M. R. Parrondo, G. P. Harmer, and D. Abbott. New paradoxical games based on Brownian ratchets. *Phys. Rev. Lett.*, 85:5226, 2000.
- [40] R. Yasuda, H. Noji, K. Kinoshita, and M. Yoshida. F_1 -Atpase is a highly efficient molecular motor that rotates with discrete 120° steps. *Cell*, 93:1117, 1998.
- [41] K. Jr. Kinoshita, R. Yasuda, H. Noji, S. Ishiwata, and M. Yoshida. F_1 -Atpase: A rotary motor made of a single molecule. *Cell*, 93:21, 1998.
- [42] R. D. Astumian. Making molecules into motors. *Sci. Am.*, 285:56, 2001.
- [43] R. D. Astumian and P. Hänggi. Brownian motors. *Phys. Today*, 55:33, 2002.
- [44] M. Rief, R. S. Rock, A. D. Mehta, M. S. Mooseker, R. E. Cheney, and J. A. Spudich. Myosin-v stepping kinetics: A molecular model for processivity. *Proc. Nat. Acad. Sci.*, 97:9482, 2000.
- [45] C. L. Asbury, A.N. Fehr, and S.M. Block. Kinesin moves by an asymmetric hand-over-hand mechanism. *Science*, 302:2130, 2003.
- [46] A. Yildiz, M. Tomishige, R. D. Vale, and P.R. Selvin. Kinesin walks hand-over-hand. *Science*, 303:676, 2004.

- [47] I. Derenyi and T. Vicsek. The kinesin walk: A dynamic model with elastically coupled heads. *Proc. Nat. Acad. Sci.*, 93:6775, 1996.
- [48] G. N. Stratopoulos, T. E. Dialynas, and G. Tsironis. Directional Newtonian motion and reversals of molecular motors. *Phys. Lett A*, 252:151, 1999.
- [49] M. Bier. Processive motor protein as an overdamped Brownian stepper. *Phys. Rev. Lett.*, 91:148104, 2003.
- [50] J. L. Mateos. Walking on ratchets with two Brownian motors. *Fluct. Noise Lett.*, 4:L161, 2004.
- [51] H. C. Fogedby, R. Metzler, and A. Svane. Exact solution of a linear molecular motor model driven by two-step fluctuations and subject to protein friction. *Phys. Rev. E.*, 70:021905, 2004.
- [52] J. L. Mateos. A random walker on a ratchet. *Physica A*, 351:79, 2005.
- [53] R. Lipowsky, S. Klumpp, and T. M. Nieuwenhuizen. Random walks of cytoskeletal motors in open and closed compartments. *Phys. Rev. Lett.*, 87:108101, 2001.
- [54] S. Klumpp and R. Lipowsky. Traffic of molecular motors through tube-like compartments. *J. Stat. Phys.*, 113:233, 2003.
- [55] M. J. I. Müller, S. Klumpp, and R. Lipowsky. Molecular motor traffic in a half open tube. *J. Phys.: Condens. Matter*, 17:S3839, 2005.
- [56] K. Visscher, M. J. Schnitzer, and S. M. Block. Single kinesin molecules studied with a molecular force clamp. *Nature*, 400:184, 1999.
- [57] M. J. Schnitzer, K. Visscher, and S. M. Block. Force production by single kinesin motors. *Nat. Cell Biol.*, 2:718, 2000.
- [58] S. Jeney, E. H. K. Stelzer, H. Grubmüller, and E. L. Florin. Mechanical properties of single motor molecules studied by three-dimensional thermal force probing in optical tweezers. *ChemPhysChem*, 5:1150, 2004.
- [59] M Karplus. Molecular dynamics of biological macromolecules: A brief history and perspective. *Biopolymers*, 68:350, 2002.
- [60] E. M. Purcell. Life at low Reynolds number. *Am. J. Phys.*, 45:3, 1976.
- [61] E. Pollak, J. Bader, B. J. Berne, and P. Talkner. Theory of correlated hops in surface diffusion. *Phys. Rev. Lett.*, 70:3299, 1993.
- [62] M. Borromeo and F. Marchesoni. Backward-to-forward jump rates on a tilted periodic substrate. *Phys. Rev. Lett.*, 84:203, 2000.

-
- [63] O. M. Braun and R. Ferrando. Role of long jumps in surface diffusion. *Phys. Rev. E.*, 65:061107, 2002.
- [64] M. Borromeo, G. Costantini, and F. Marchesoni. Critical hysteresis in a tilted washboard potential. *Phys. Rev. Lett.*, 82:2820, 1999.
- [65] G. Costantini and F. Marchesoni. Threshold diffusion in a tilted washboard potential. *Europhys. Lett.*, 48:491, 2000.
- [66] O. M. Braun, A. R. Bishop, and J. Röder. Hysteresis in the underdamped driven Frenkel-Kontorova model. *Phys. Rev. Lett.*, 79:3692, 1997.
- [67] C. Cattuto and F. Marchesoni. Unlocking of an elastic string from a periodic substrate. *Phys. Rev. Lett.*, 79:5070, 1997.
- [68] E. Ben-Jacob, D. J. Bergman, B. J. Matkowsky, and Z. Schuss. Lifetime of oscillatory steady states. *Phys. Rev. A.*, 26:2805, 1982.
- [69] E. Ben-Jacob, D. J. Bergman, and Z. Schuss. Thermal fluctuations and lifetime of the nonequilibrium steady state in a hysteretic Josephson junction. *Phys. Rev. B.*, 25:519, 1982.
- [70] R. Bartussek, P. Hänggi, and J. G. Kissner. Periodically rocked thermal ratchets. *Europhys. Lett.*, 28:459, 1994.
- [71] S. Savel'ev, F. Marchesoni, P. Hänggi, and F. Nori. Nonlinear signal mixing in a ratchet device. *Europhys. Lett.*, 67:179, 2004.
- [72] S. Savel'ev, F. Marchesoni, P. Hänggi, and F. Nori. Transport via nonlinear signal mixing in ratchet devices. *Phys. Rev. E.*, 70:066109, 2004.
- [73] P. Hänggi and R. Bartussek. Brownian rectifiers: How to convert Brownian motion into directed transport. *Lect. Notes Phys.*, 476:294, 1996.
- [74] R. D. Astumian. Thermodynamics and kinetics of a Brownian motor. *Science*, 276:917, 1997.
- [75] P. Reimann and P. Hänggi. Introduction to the physics of Brownian motors. *Appl. Phys. A: Mater. Sci. Process.*, 75:169, 2002.
- [76] H. Linke, editor. *Ratchets and Brownian motors: Basics, experiments and applications*, *Appl. Phys. A: Mater. Sci. Process.* volume 75, 2002.
- [77] P. Jung, J. G. Kissner, and P. Hänggi. Regular and chaotic transport in asymmetric periodic potentials: Inertia ratchets. *Phys. Rev. Lett.*, 76:3436, 1996.

- [78] L. Machura, M. Kostur, P. Talkner, J. Łuczka, F. Marchesoni, and P. Hänggi. Brownian motors: Current fluctuations and rectification efficiency. *Phys. Rev. E.*, 70:061105, 2004.
- [79] D. Suzuki and T. Munakata. Rectification efficiency of a Brownian motor. *Phys. Rev. E.*, 68:021906, 2003.
- [80] E. Pécelet. *Ann. Chim. Phys.*, 3:107, 1841.
- [81] E. Pécelet. *Traité de la Chaleur Considérée dans ses Applications*, volume 3. Hachette, Paris, 1843.
- [82] L. Machura, M. Kostur, F. Marchesoni, P. Talkner, P. Hänggi, and J. Łuczka. Optimal strategy for controlling transport in inertial Brownian motors. *J. Phys.: Condens. Matter*, 17:S3741–S3752, 2005.
- [83] B. Lindner, M. Kostur, and L. Schimansky-Geier. Optimal diffusive transport in a tilted periodic potential. *Fluct. Noise Lett.*, 1:R25, 2001.
- [84] B. Lindner, L. Schimansky-Geier, P. Reimann, P. Hänggi, and M. Nagaoka. Inertia ratchets: A numerical study versus theory. *Phys. Rev. E.*, 59:1417, 1999.
- [85] P. Hänggi and H. Thomas. Stochastic processes: Time-evolution, symmetries and linear response. *Phys. Rep.*, 88:207, 1982.
- [86] H. Wang. Chemical and mechanical efficiencies of molecular motors and implications for motor mechanisms. *J. Phys.: Condens. Matter*, 17:S3997, 2005.
- [87] R. L. Honeycutt. Stochastic Runge-Kutta algorithms. I. White noise. *Phys. Rev. A.*, 45:600, 1992.
- [88] H. Linke, M. T. Downton, and M. J. Zuckermann. Performance characteristic of Brownian motors. *Chaos*, 15:026111, 2005.
- [89] L. D. Landau and E. M. Lifshitz. *Fluid Dynamics*. Pergamon Press, Oxford, 1959.
- [90] H. X. Zhou and Y. D. Chen. Chemically driven motility of Brownian particles. *Phys. Rev. Lett.*, 77:194, 1996.
- [91] K. Sekimoto. Kinetic characterization of heat bath and the energetics of thermal ratchet mode. *J. Phys. Soc. Jpn.*, 66:1234, 1997.
- [92] H. Wang and G. Oster. The Stokes efficiency for molecular motors and its applications. *Europhys. Lett.*, 57:134, 2002.
- [93] H. Kamegawa, T. Hondou, and F. Takagi. Energetics of a forced thermal ratchet. *Phys. Rev. Lett.*, 80:5251, 1998.

-
- [94] I. M. Sokolov and A. Blumen. Thermodynamical and mechanical efficiency of a ratchet pump. *Chem. Phys.*, 235:39, 1998.
- [95] J. M. R. Parrondo, J. M. Blanco, F. J. Cao, and R. Brito. Efficiency of brownian motors. *Europhys. Lett.*, 43:248, 1998.
- [96] I. Derenyi, M. Bier, and R. D. Astumian. Generalized efficiency and its application to microscopic engines. *Phys. Rev. Lett.*, 83:903, 1999.
- [97] A. Parmeggiani, F. Jülicher, A. Ajdari, and J. Prost. Energy transduction of isothermal ratchets: Generic aspects and specific examples close to and far from equilibrium. *Phys. Rev. E.*, 60:2127, 1999.
- [98] K. Sekimoto, F. Takagi, and T. Hondou. Carnot's cycle for small systems: Irreversibility and cost of operations. *Phys. Rev. E.*, 62:7759, 2000.
- [99] J. M. R. Parrondo and B. J. de Cisneros. Energetics of brownian motors: A review. *Appl. Phys. A: Mater. Sci. Process.*, 75:179, 2002.
- [100] M. Asfaw and M. Bekele. Current, maximum power and optimized efficiency of a brownian heat engine. *Eur. J. Phys. B*, 38:457, 2004.
- [101] D. Suzuki and T. Munakata. Rectification efficiency of the Feynman ratchet. *J. Phys. Soc. Jpn.*, 74:550, 2005.
- [102] T. Harada. Phenomenological energetics for molecular motor. *Europhys. Lett.*, 70:49, 2005.
- [103] J. L. Mateos. Chaotic transport and current reversal in deterministic ratchets. *Phys. Rev. Lett.*, 84:258, 2000.
- [104] M. Barbi and M. Salerno. Phase locking effect and current reversals in deterministic underdamped ratchets. *Phys. Rev. E.*, 62:1988, 2000.
- [105] M. Porto, M. Urbakh, and J. Klafter. Molecular motor that never steps backwards. *Phys. Rev. Lett.*, 85:491, 2000.
- [106] S. Flach, O. Yevtushenko, and Y. Zolotaryuk. Directed current due to broken time-space symmetry. *Phys. Rev. Lett.*, 84:2358, 2000.
- [107] J. L. Mateos. Current reversals in chaotic ratchets. *Acta. Phys. Pol. B*, 32:307, 2001.
- [108] C. M. Arizmendi, F. Family, and A. L. Salas-Brito. Quenched disorder effects on deterministic inertia ratchets. *Phys. Rev. E.*, 63:061104, 2001.
- [109] J. L. Mateos. Current reversals in deterministic ratchets: Points and dimers. *Physica D*, 168-169:205, 2002.

- [110] M. Borromeo, G. Costantini, and F. Marchesoni. Deterministic ratchets: Route to diffusive transport. *Phys. Rev. E.*, 65:041110, 2002.
- [111] H. A. Larrondo, F. Family, and C. M. Arizmendi. Control of current reversal in single and multiparticle inertia ratchets. *Physica A*, 303:67, 2002.
- [112] J. L. Mateos. Current reversals in chaotic ratchets: The battle of attractors. *Physica A*, 325:92, 2003.
- [113] H. A. Larrondo, C. M. Arizmendi, and F. Family. Current basins of attraction in inertia ratchets. *Physica A*, 320:119, 2003.
- [114] S. Sengupta, R. Guantes, S. Miret-Artes, and P. Hänggi. Controlling directed transport in two-dimensional periodic structures under crossed electric fields. *Physica A*, 338:406, 2004.
- [115] F. Family, H. A. Larrondo, D. G. Zarlenga, and C. M. Arizmendi. Chaotic dynamics and control of deterministic ratchets. *J. Phys.: Condens. Matter*, 17:S3719, 2005.
- [116] W. S. Son, I. Kim, Y. J. Park, , and C. M. Kim. Current reversal with type-I intermittency in deterministic inertia ratchets. *Phys. Rev. E.*, 68:067201, 2003.
- [117] B. Hu and J. Rudnick. Exact solutions to the Feigenbaum renormalization-group equations for intermittency. *Phys. Rev. Lett.*, 48:1645, 1982.
- [118] P. Jung and P. Hänggi. Invariant measure of a driven nonlinear oscillator with external noise. *Phys. Rev. A.*, 41:2977, 1990.
- [119] M. Schreier, P. Reimann, P. Hänggi, and E. Pollak. Giant enhancement of diffusion and particle selection in rocked periodic potentials. *Europhys. Lett*, 44:416, 1998.
- [120] P. Reimann, C. Van den Broeck, H. Linke, P. Hänggi, J. M. Rubi, and A. Pérez-Madrid. Giant acceleration of free diffusion by use of tilted periodic potentials. *Phys. Rev. Lett.*, 87:010602, 2001.
- [121] P. Reimann, C. Van den Broeck, H. Linke, P. Hänggi, J. M. Rubi, and A. Pérez-Madrid. Diffusion in tilted periodic potentials: Enhancement, universality, and scaling. *Phys. Rev. E.*, 65:031104, 2002.
- [122] M. Kostur, L. Machura, P. Hänggi, J. Łuczka, and P. Talkner. Forcing inertial Brownian motors: Efficiency and negative differential mobility. *accepted to Phys. Rev. E*, 2006.
- [123] M. Kostur, L. Machura, P. Hänggi, J. Łuczka, and P. Talkner. Absolute negative mobility in inertial tilted periodic potential. *unpublished*, 2006.
- [124] F. Nava, C. Canali, F. Catellani, G. Gavioli, and G. Ottaviani. Electron-drift velocity in high-purity ge between 8 and 240 k. *J. Phys. C: Solid State Phys.*, 9:1685, 1976.

-
- [125] L. Hartmann, M. Grifoni, and P. Hänggi. Dissipative transport in dc-ac driven tight binding lattices. *Europhys. Lett*, 38:497, 1997.
- [126] C. Van den Broeck, I. Bena, P. Reimann, and J. Lehmann. Coupled Brownian motors on a tilted washboard. *Ann. Phys. (Leipzig)*, 9:713, 2000.
- [127] C. Van den Broeck, B. Cleuren, R. Kawai, and M. Kambon. A Trio of Brownian Donkeys. *International Journal of Modern Physics C*, 13:1195, 2002.
- [128] R. Eichhorn and P. Reimann. Meandering Brownian donkeys. *Acta. Phys. Pol. B*, 35:1407, 2004.
- [129] S. R. White and M. Barma. Field-induced drift and trapping in percolation networks. *J. Phys. A*, 17:2995, 1984.
- [130] V. Balakrishnan and C. Van den Broeck. Transport properties on a random comb. *Physica A*, 217:1, 1995.
- [131] G. A. Cecchi and M. O. Magnasco. Negative resistance and rectification in Brownian transport. *Phys. Rev. Lett.*, 76:1968, 1996.
- [132] G. W. Slater, H. L. Guo, and G. I. Nixon. Bidirectional transport of polyelectrolytes using self-modulating entropic ratchets. *Phys. Rev. Lett.*, 78:1170, 1997.
- [133] R. Eichhorn, P. Reimann, and P. Hänggi. Brownian motion exhibiting absolute negative mobility. *Phys. Rev. Lett.*, 88:190601, 2002.
- [134] R. Eichhorn, P. Reimann, and P. Hänggi. Paradoxical motion of a single Brownian particle: Absolute negative mobility. *Phys. Rev. E.*, 66:066132, 2002.
- [135] B. Cleuren and C. Van den Broeck. Random walks with absolute negative mobility. *Phys. Rev. E.*, 65:030101, 2002.
- [136] A. Haljas, R. Mankin, A. Sauga, and E. Reiter. Anomalous mobility of Brownian particles in a tilted symmetric sawtooth potential. *Phys. Rev. E.*, 70:041107, 2004.
- [137] I. Zapata, R. Bartussek, F. Sols, and P. Hänggi. Voltage rectification by SQUID ratchet. *Phys. Rev. Lett.*, 77:2292, 1996.
- [138] T. Dittrich, R. Ketzmerick, M. F. Otto, and H. Schanz. Classical and quantum transport in deterministic hamiltonian ratchets. *Ann. Phys. (Leipzig)*, 9:755, 2000.
- [139] S. Denisov and S. Flach. Dynamical mechanisms of dc current generation in driven Hamiltonian systems. *Phys. Rev. E.*, 64:056236, 2001.
- [140] H. Schanz, M. F. Otto, R. Ketzmerick, and T. Dittrich. Classical and quantum Hamiltonian ratchets. *Phys. Rev. Lett.*, 87:070601, 2001.

Bibliography

Acknowledgments

First of all, I would like to thank Prof. Dr. Peter Hänggi for giving me a possibility of working in his group, for his constant support during all these years in Augsburg.

My whole adventure with the science, in particular with the physics of ratchets would not be possible without Prof. Dr. Jerzy Łuczka. I am grateful for his introduction to this fascinating topic, for talks and lectures, and always having time for solving my problems.

I am also very thankful to Prof. Dr. Peter Talkner for his dedicated support, always objective, precise answering my questions and also for reading and improvement of this manuscript.

Many thanks go to Dr. Marcin Kostur for our never ending and fruitful talks (though not always on physics), his complaining and arguing, but, the most important, for his friendship.

I appreciate all of the constructive discussions with Dr. Gerhard Schmid and all his comments to this thesis.

I would like to express my gratitude to Prof. Dr. Jose Mateos for his remarks and explanation of the deterministic dynamics of the rocking ratchets.

I would like to thank every single member of the group of the Theoretical Physics I at the University of Augsburg for a very motivating and comfortable atmosphere.

I gratefully acknowledge the financial support by the Graduiertenkolleg GRK 283 “Nichtlineare Probleme in Analysis, Geometrie und Physik” and the year DAAD grant.

At last, but not least, I would like to thank my parents for their constant support and my education. Special thanks go to my wife Ania and daughter Agata for their love and patience.

Curriculum Vitae

Łukasz Machura

Date of Birth: 1 December 1977

Place of Birth: Zawiercie, Poland

Status: Married, one daughter

Parents: Julian and Stefania Machura

EDUCATION:

- 1984-1992 Primary School, Zawiercie, Poland.
- 1992-1996 High School, the biological-chemical profile, Zawiercie, Poland.
- 1996-1999 general physics study, University of Silesia, Katowice, Poland.
- 1999-2001 theoretical physics study, The Department of Theoretical Physics, University of Silesia, Katowice, Poland.
- 2001 MSc in theoretical physics (stochastic processes), thesis: "Inertial Effects In Dichotomic Ratchets", advisor: Prof. Dr. Jerzy Łuczka.
- 2001-2002 Ph.D. study, Department of Theoretical Physics, University of Silesia, Katowice, Poland.
- 2002-2003 research in the group of Prof. Dr. Peter Hänggi, Augsburg University, Germany – a year DAAD grant.
- 2003-2006 Ph.D. study, Theoretical Physics I, Augsburg University, Germany – a three year Graduiertenkolleg 283 scholarship.

MEMBERSHIP: Polish Physical Society.